Electronic Supplementary Material (ESI) for Journal of Materials Chemistry C.

SUPPLEMENTARY INFORMATION

Functionalised Al(III) metal organic frameworks for fluorescence sensing of nitroaromatic vapours

Amina Haj-Yahya,[a] Dimitra Kouskouki,[a] Antigoni G. Margellou,[a] Evangelos K. Andreou,[b] Gerasimos S. Armatas,[b] Theodore Lazarides*[a]

[a] Department of Chemistry, Aristotle University of Thessaloniki, 54124, Thessaloniki, Greece
E-mail: tlazarides@chem.auth.gr

[b] Department of Materials Science and Technology, University of Crete, Vassilika Vouton, Heraklion 70013, Greece

Table of Contents

Materials and Methods

All starting materials, solvents and analytes were used as received from the usual commercial sources (Sigma Aldrich, Alfa Aesar). Ligand **L–1** was prepared according to a synthetic process we have previously reported.[1]

Physical Methods

The ^{1}H-NMR spectra were recorded at room temperature on an Agilent 500 MHz NMR spectrometer with the use of deuterated solvents D_2O and NaOD (1.0 M). IR spectra were recorded in a scan range from 400 to 4000 cm^{-1} on a Nicolet FT-IR 6700 spectrophotometer equipped with a diamond attenuated total reflection (ATR) stage. Powder X-ray diffraction (PXRD) measurements were performed at room temperature on a Bruker D8 Advance powder X-ray diffractometer with Cu-Ka radiation (k = 1.5418 Å). Thermogravimetric analysis (TGA) was performed on a STA 449 F5 Jupiter instrument under air atmosphere with a heating rate of 5 °C min^{-1}. Nitrogen sorption studies were performed at 77 K with a Quantachrome NOVA 3200e sorption analyzer (Quantachrome Instruments), after sample degassing at 150 °C for 12 h, and surface areas were calculated according to the Brunauer–Emmett–Teller (BET) method.[2] The UV–vis spectra of nitroaromatic were measured on a Hitachi-2001 spectrophotometer in the wavelength range of 250–450 nm. The fluorescence spectra were measured on an Edinburgh Instruments FS5 spectrofluorometer equipped with a red-sensitive Hamamatsu R13456 photomultiplier tube (PMT) using a 150 W Xenon arc lamp as light source. All spectra were corrected for detector response by using the correction files and software (Fluoracle) provided by the manufacturer. Emission quantum yields were measured using the SC–30 integrating sphere module that consists of a 150 mm inner diameter spherical cavity, constructed from PTFE–based material. Calculation of the quantum yields were carried out using a designated routine within the Fluoracle software according to the equation (S1) utilizing the emission spectra of the studied sample and a reference sample. Appropriate corrections were applied as provided by the manufacturer.

$$\Phi = \frac{Sample\ Emission\ Area - Reference\ Emission\ Area}{Reference\ Scattering - Sample\ scattering} \quad \textbf{(S1)}$$

Nanosecond time-resolved experiments were performed in an Edinburgh Instruments mini-τ lifetime spectrometer using a bandpass filter (FWHM = 50 nm) at 500 nm. The excitation source was an Edinburgh Instruments picosecond pulsed LED (EPLED-320) with a peak wavelength 326.8 nm and pulse width 910 ps. The detector was a thermoelectrically cooled, high-speed red-sensitive photomultiplier tube (Hamamatsu H10720-01). Instrument response function (IRF) was collected using a sample consisting of water with a few drops of colloidal silica (LUDOX™-Aldrich) scattering medium in an open filter configuration. The data were analysed using the software (FluoracleTM) provided by the manufacturer.

Compound preparation

Al^{3+} MOFs were synthesized following a typical solvothermal method.[3–5] $AlCl_3 \cdot 6H_2O$ (44 mg, 0.18 mmol) and the corresponding amounts of **L–1** and H_2bdc given in Table 1 were added in deionised H_2O (9 mL) and DMF (1 mL) in 23 mL Teflon vials. The vials were heated inside stainless-steel Parr bombs to 120 °C under autogenous pressure for 24 h and subsequently cooled to room temperature. The reactions yielded yellow to pale-yellow solids that were separated by centrifugation and washed thoroughly with DMF. Afterwards, the products were soaked in DMF (2 mL) for 3 days at room temperature, during which time the supernatant was removed and fresh DMF was added each day. This process was carried out to wash out residual reagents that may be trapped inside the material's pores. The DMF molecules were exchanged by soaking in MeOH with three additions of fresh MeOH over 3 days, followed by heating the compounds soaked in MeOH at 50 °C for 24 hr. Finally, the solid samples were isolated by centrifugation and air-dried to yield ~40 mg of each product. IR (cm^{-1}): **Al–1**: 3404 b, 1575 s, 1507 w, 1469 m, 1443 s, 1424 m, 1402 s, 1311 w, 1279 w, 992 m, 770 m, 603 b, 549 w, 466 w. **Al–0.5**: 3421 b, 1595 s, 1509 m, 1442 s, 1417 s, 1287 b, 989 m, 769 w, 753 w, 598 w, 472 w. **Al–0.25**: 3421 b, 1599 s, 1580 s, 1510 m, 1443, m, 1418 s, 1285 b, 1104 b, 998 m, 754 m, 599 m, 457 w.

Table S1. *Corresponding ammounts of* ***L–1*** *and* H_2*bdc used in MOF syntheses.*

MOF name	MOF formula	**L–1**	H_2bdc
Al–1	{Al(OH)(**L–1**)}	44.8 mg (0.16 mmol)	**–**
Al–0.5	{Al(OH)$(bdc)_{0.5}$(**L–1**)$_{0.5}$}	22.4 mg (0.08 mmol)	13.8 mg (0.08 mmol)
Al–0.25	{Al(OH)$(bdc)_{0.75}$(**L–1**)$_{0.25}$}	11.2 mg (0.04 mmol)	20.4 mg (0.12 mmol)

Film preparation

Film fabrication was based on the combination of MOF powder with a few percentages of a bio-sourced binder derived from cellulose (Hydroxyethyl cellulose, HEC), following a simple method reported in literature.[6] Firstly, we formed a MOF-based paste by mixing 10 mg of MOF powder with *ca.* 1 g of a gel containing HEC 1.5%wt. The mixture was thoroughly kneaded with the use of a pestle and mortar to afford a homogenous paste. Approximately 5 mg of the mixture was uniformly applied on each cover glass slide (10 mm × 30 mm). The coated glasses were thermally activated at 120 °C for 24 h prior to fluorescence measurements, as described in following sections.

NMR spectroscopy

The relative percentages of **L–1** and bdc^{2-} incorporated in the MOFs' structures was determined by ^{1}H-NMR study of digested materials in D_2O/NaOD. The peaks corresponding to **L–1** are found at *ca.* δ (ppm) 7.50, 7.16, 7.13, 7.03, 6.97, 6.85 and 4.20 and the peak of bdc^{2-} is found at *ca.* δ (ppm) 7.60. The mol% of ligand **L–1** was estimated following the formula:

$$mol\% = \frac{\frac{I_{L-1}}{n_{L-1}}}{\frac{I_{L-1}}{n_{L-1}} + \frac{I_{bdc}}{n_{bdc}}} \times 100 \quad \textbf{(S2)}$$

where I is the peak integral and *n* is the number of protons attributed to the corresponding peak. We applied the integration data from the ^{1}H-NMR spectra of **Al–0.5** and **Al–0.25** (shown below) on the equation S2 and the mol% **L–1** value was estimated to 50% and 25%, respectively, in agreement with experimental parameters.

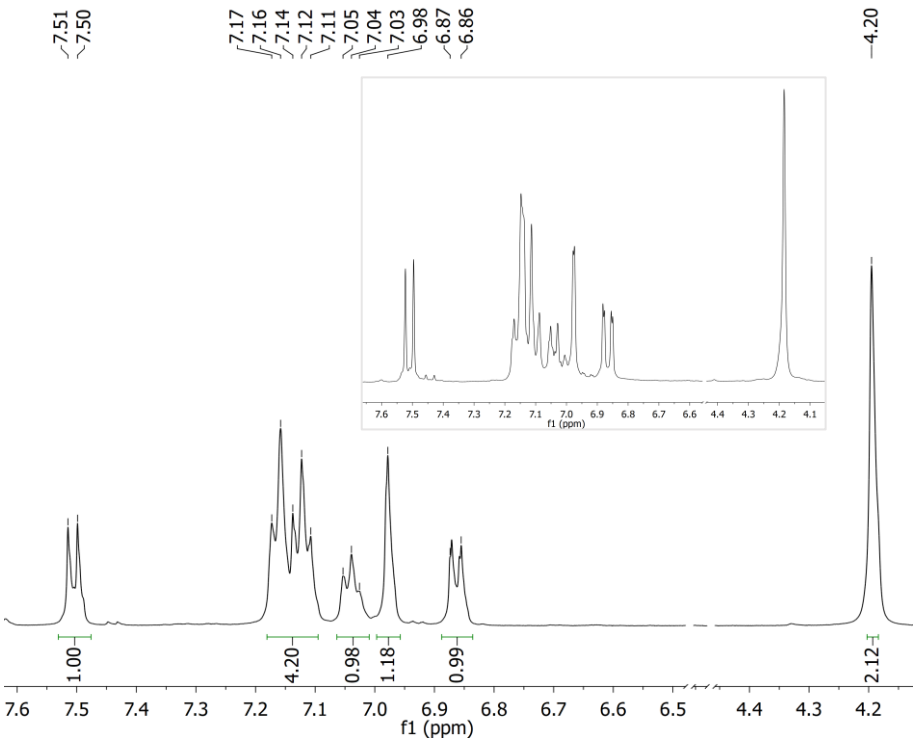

Figure S1. *^{1}H-NMR spectrum of **Al–1** digested in D_2O/NaOD. Inset: ^{1}H-NMR spectrum of **Al–1** activated at 120 °C for 24 hr digested in D_2O/NaOD.*

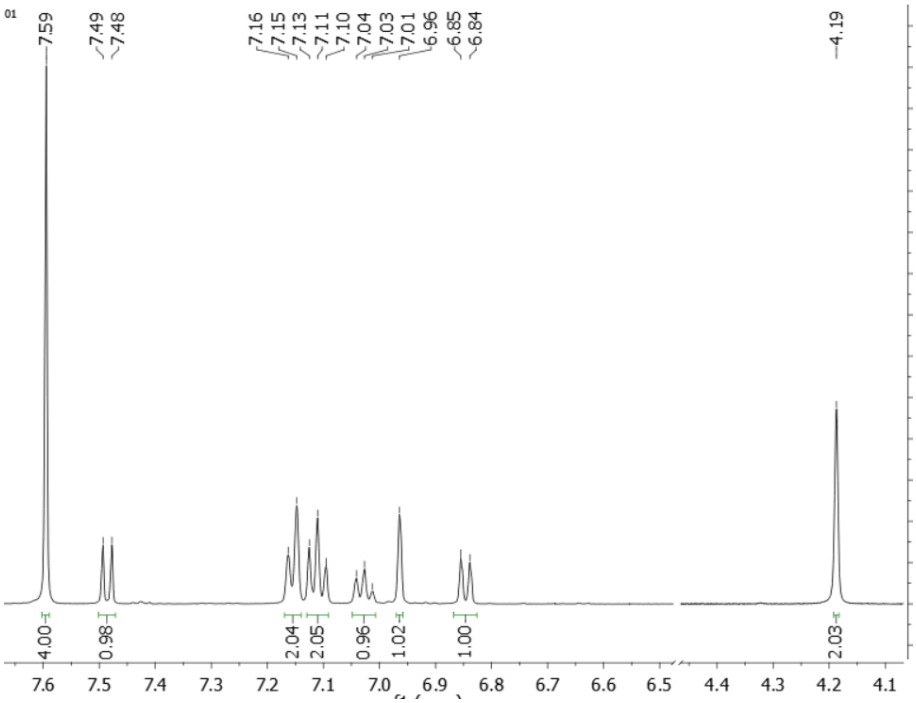

Figure S2. *^{1}H-NMR spectrum of **Al–0.5** digested in D_2O/NaOD.*

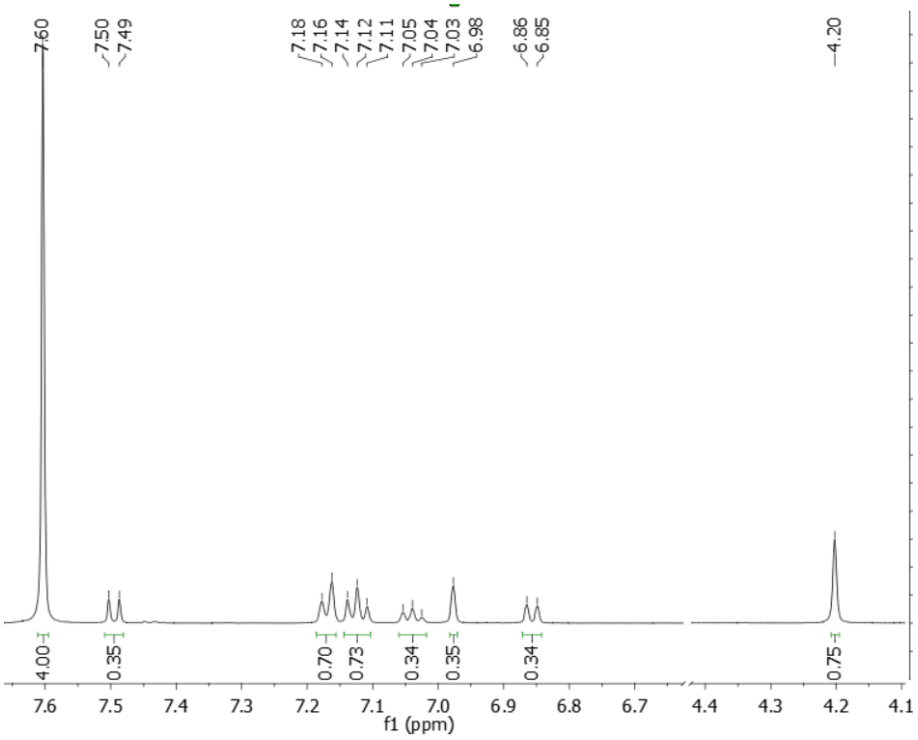

Figure S3. *^{1}H-NMR spectrum of **Al–0.25** digested in D_2O/NaOD.*

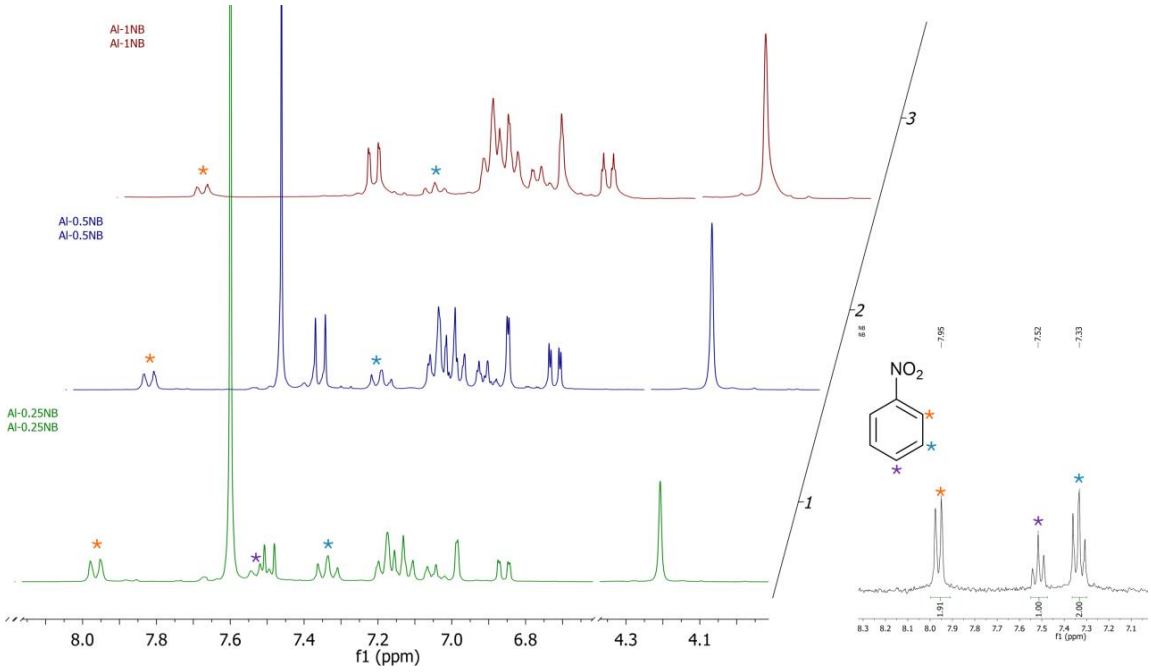

Figure S4. *^{1}H-NMR spectra of MOF samples **Al–1** (red), **Al–0.5** (blue), **Al–0.25** (green) after exposure to vapours of NB and NB (aromatic region) in D_2O/NaOD along with a proton numbering scheme of NB.*

IR spectroscopy

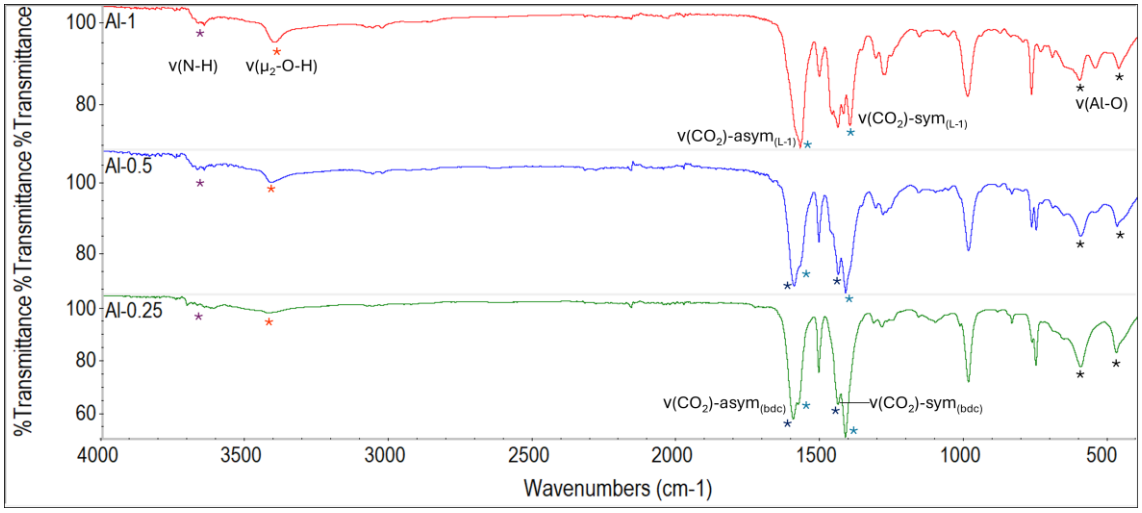

***Figure S5**. IR spectra of **Al–1** (red), **Al–0.5** (blue), **Al–0.25** (green).*

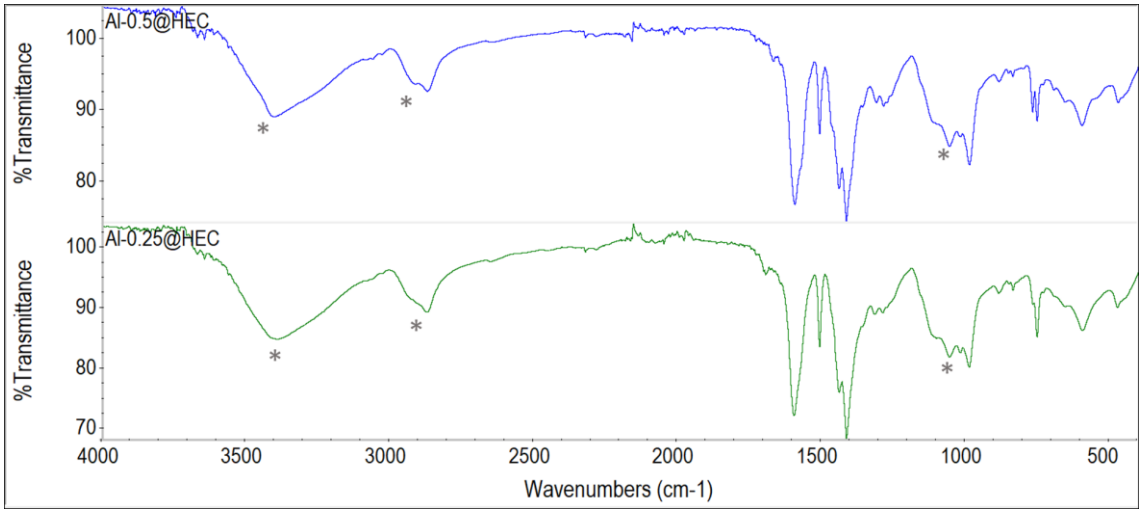

***Figure S6.** IR spectra of **Al–0.5@HEC** (blue) and **Al–0.25@HEC** (green).*

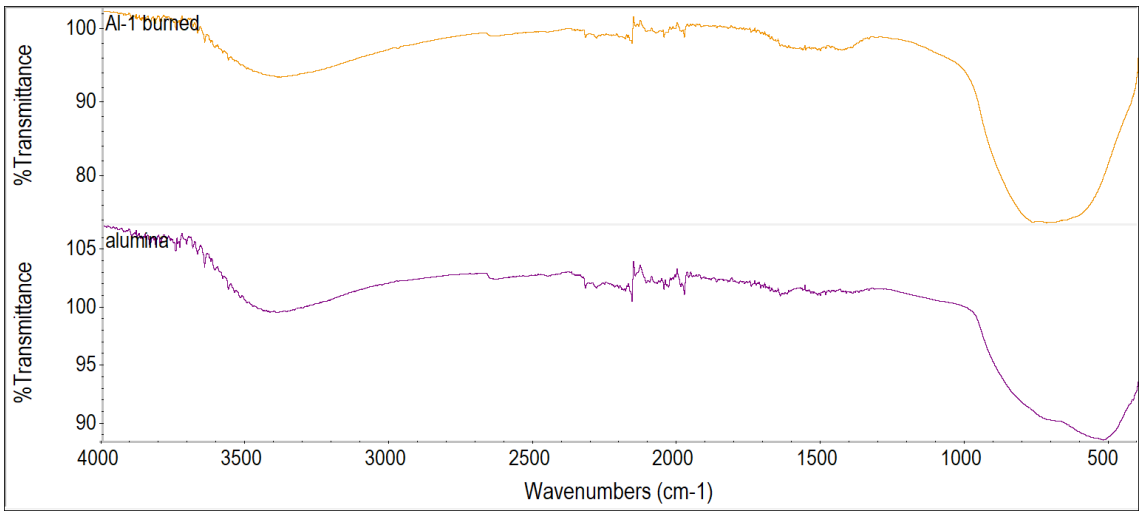

Figure S7. *IR spectra of* ***Al–1*** *thermally treated at 600 °C (orange) and Al_2O_3 (purple).*

PXRD patterns and Le Bail refinements

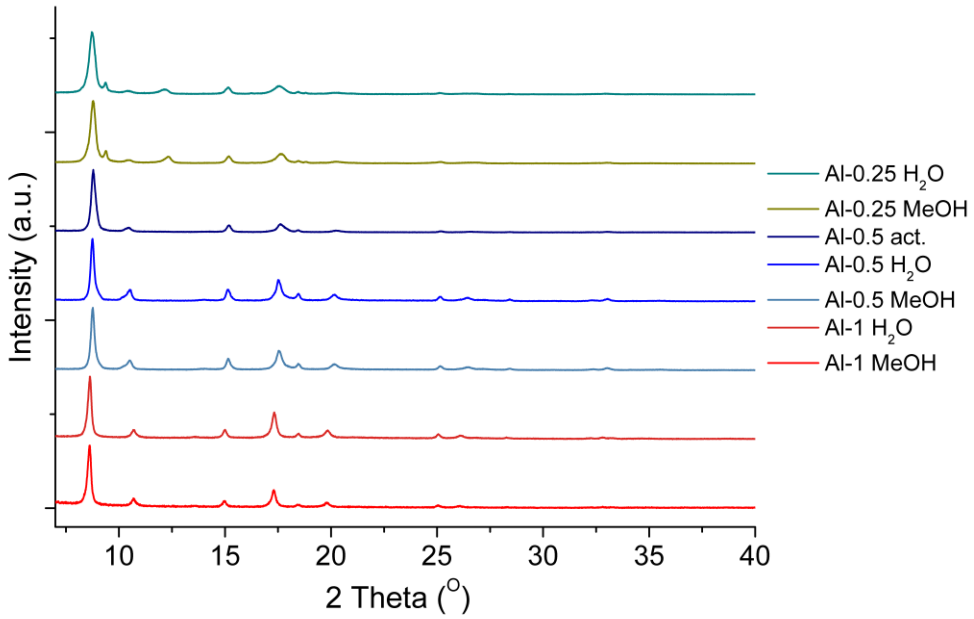

Figure S8. *PXRD patterns of* ***Al–1, Al–0.5*** *and* ***Al–0.25*** *after MeOH and H_2O treatment for 24 h and* ***Al–0.5*** *after activation at 120 °C for 24 hr.*

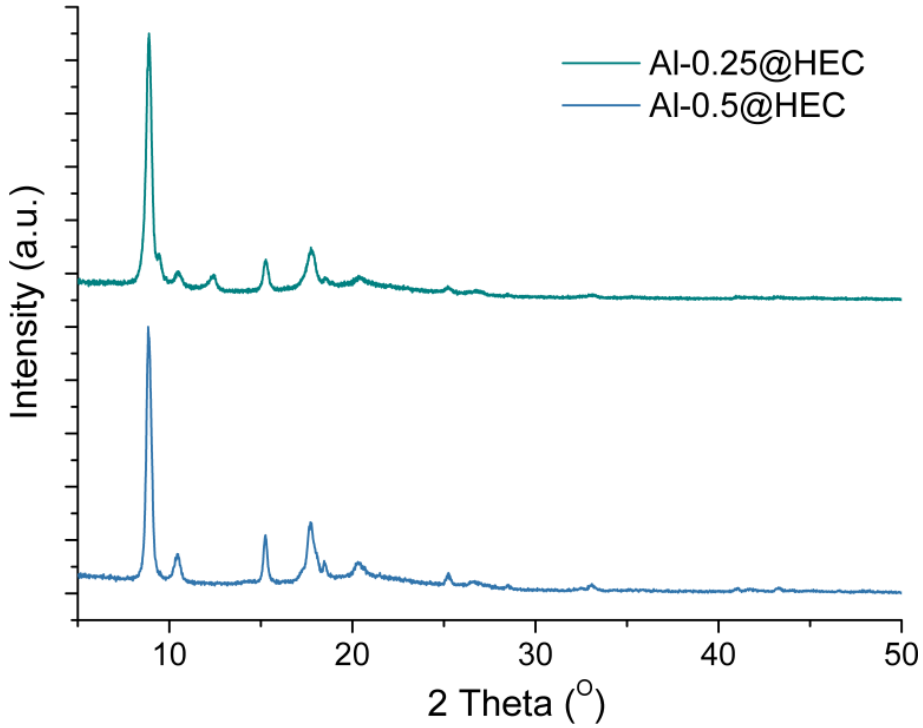

Figure S9. *PXRD patterns of* ***Al–0.5@HEC*** *(blue) and* ***Al–0.25@HEC*** *(green).*

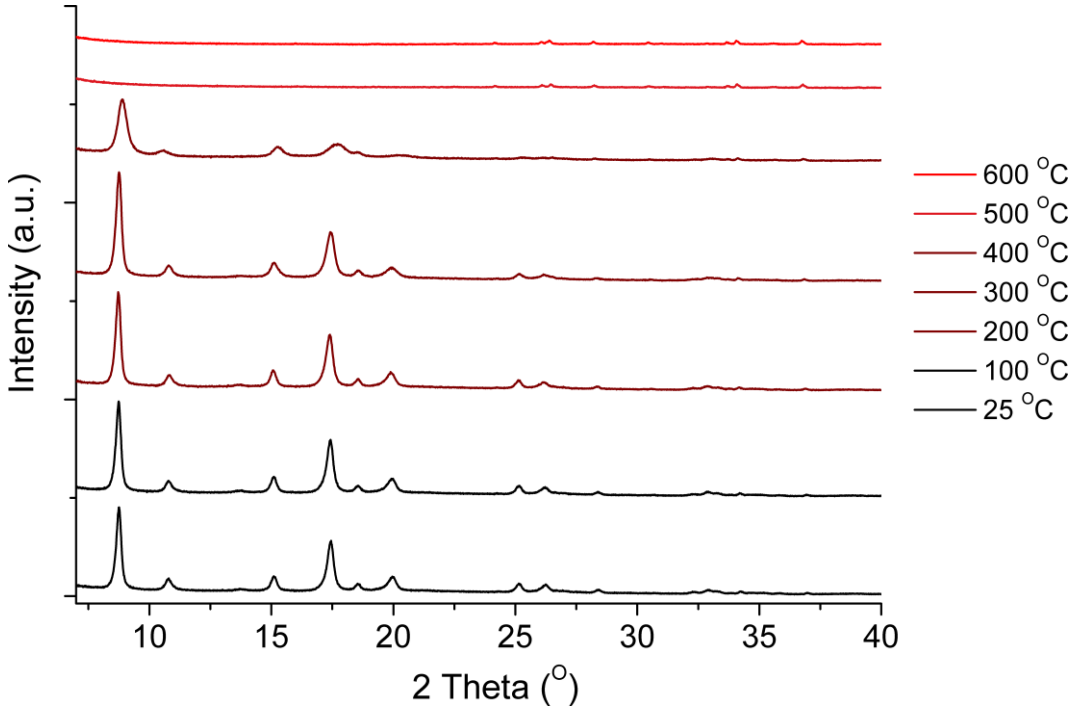

Figure S10. *TDPXRD patterns of* ***Al–1*** *from 25 to 600 °C in steps of 100 °C.*

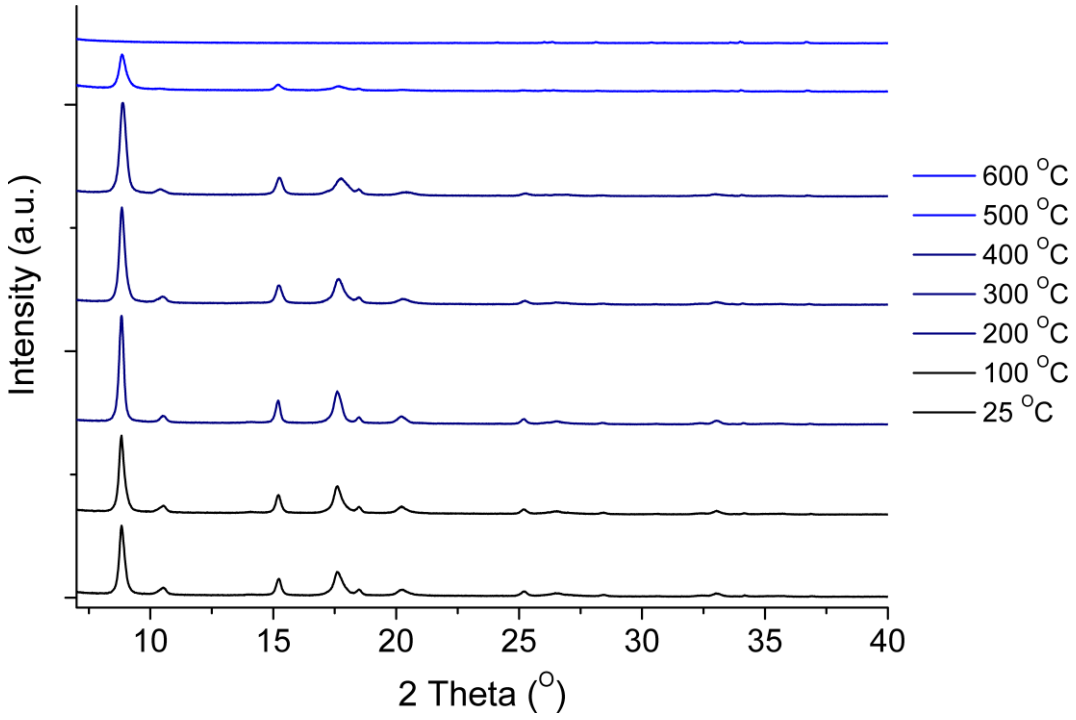

Figure S11. *TDPXRD patterns of* ***Al–0.5*** *from 25 to 600 °C in steps of 100 °C.*

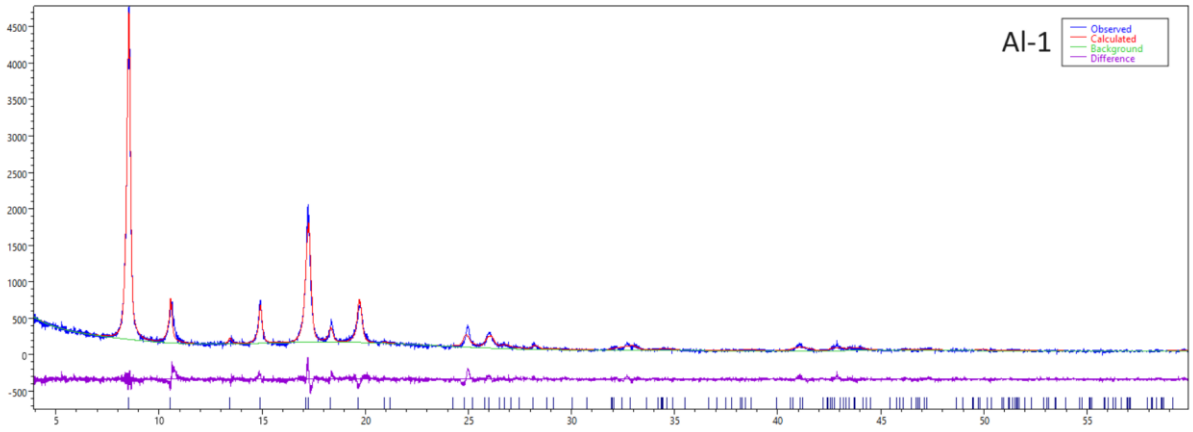

Figure S12. *Le Bail refinement of* ***Al–1*** *over MIL–53 open-pore structure*[7]*. Agreement factors:* R_p *= 7.985,* R_{wp} *= 10.913. Blue line: experimental pattern; red line: calculated pattern; purple line: difference pattern (exp. – calc.); green line: background; navy bars: Bragg positions.*

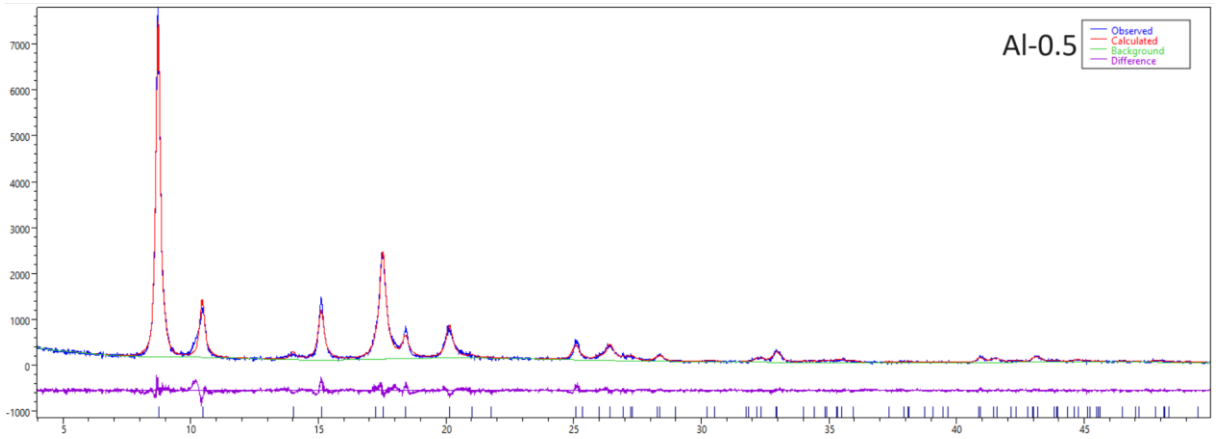

Figure S13. *Le Bail refinement of* ***Al–0.5*** *over MIL–53 open-pore structure*[7]*. Agreement factors:* R_p *= 7.352,* R_{wp} *= 10.074. Blue line: experimental pattern; red line: calculated pattern; purple line: difference pattern (exp. – calc.); green line: background; navy bars: Bragg positions.*

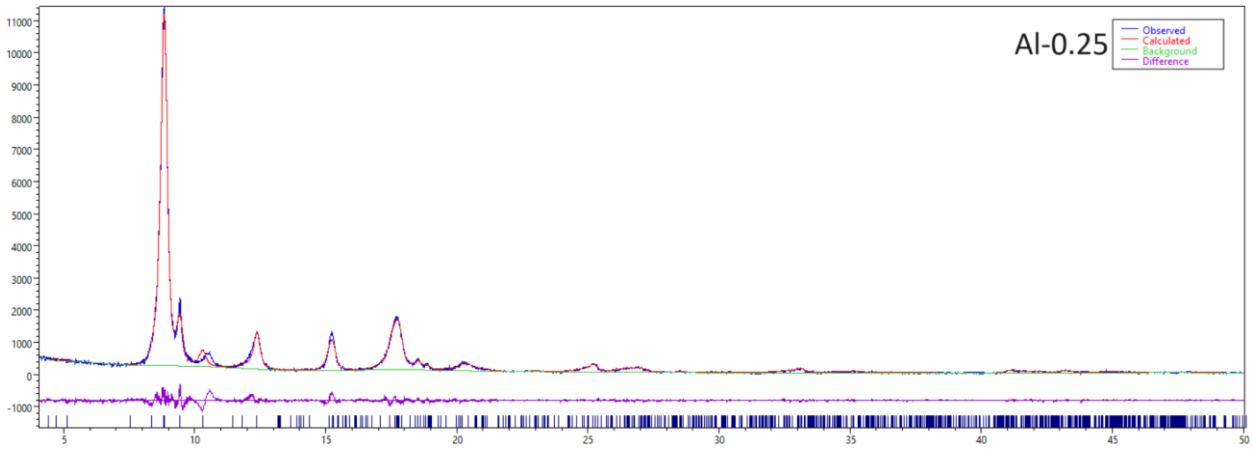

Figure S14. *Le Bail refinement of* ***Al–0.25*** *fitted to a* NH_2*–MIL–53 MOF showing a monoclinic distortion*[8]*. Agreement factors:* R_p *= 6.680,* R_{wp} *= 10.393. Blue line: experimental pattern; red line: calculated pattern; purple line: difference pattern (exp. – calc.); green line: background; navy bars: Bragg positions.*

TG analysis

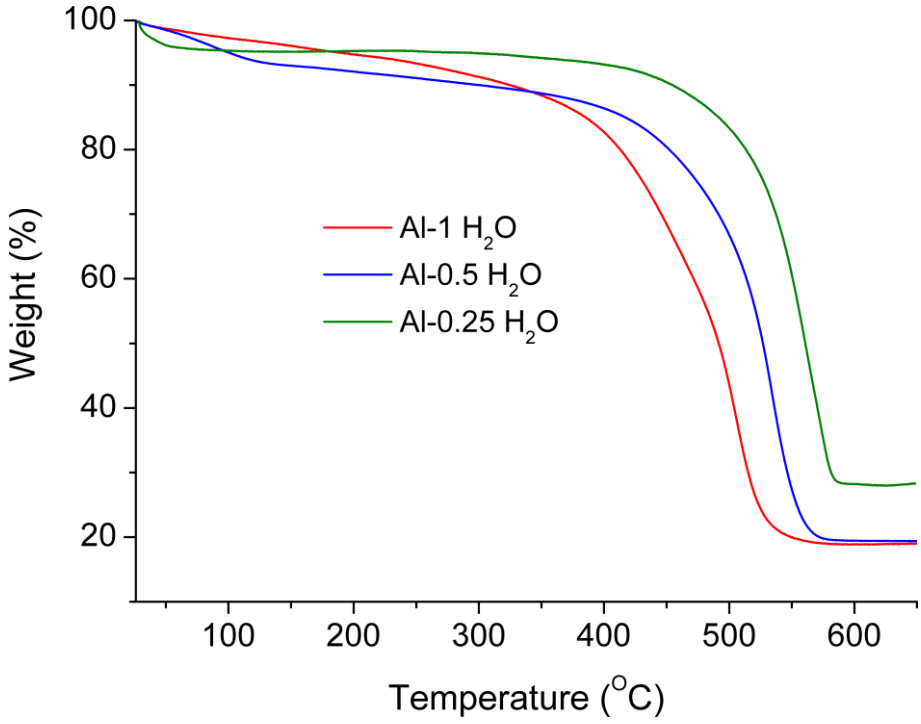

Figure S15. *TGA curves for* ***Al–1*** *(red),* ***Al–0.5*** *(blue) and* ***Al–0.25*** *(green) after H_2O treatment, under air flow.*

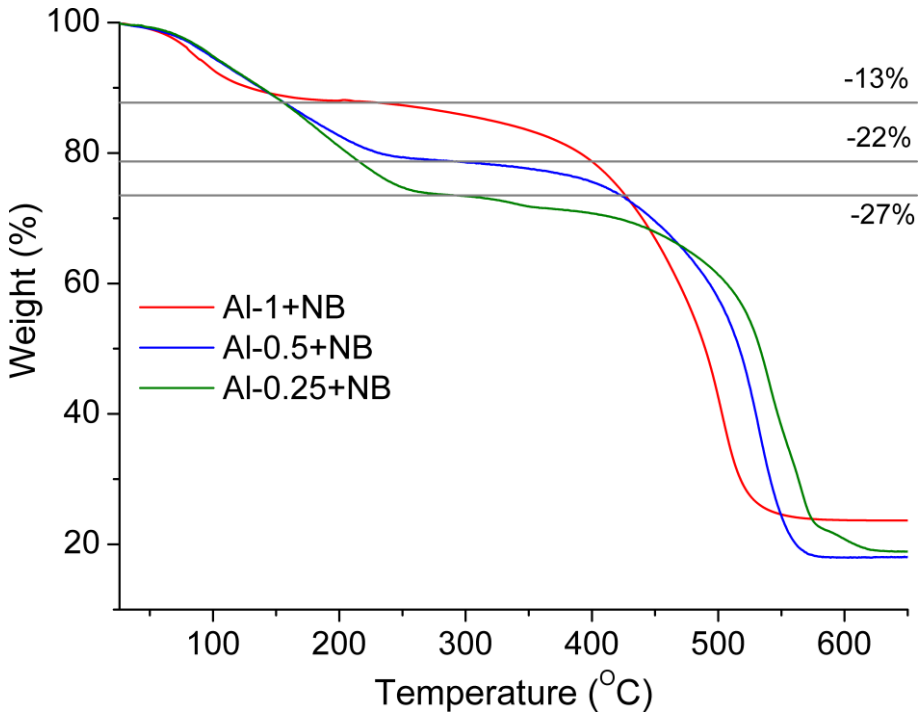

Figure S16. *TGA curves for* ***Al–1*** *(red),* ***Al–0.5*** *(blue) and* ***Al–0.25*** *(green) under air flow, after MeOH treatment and exposure to NB vapours for 3 days.*

Fluorescence properties

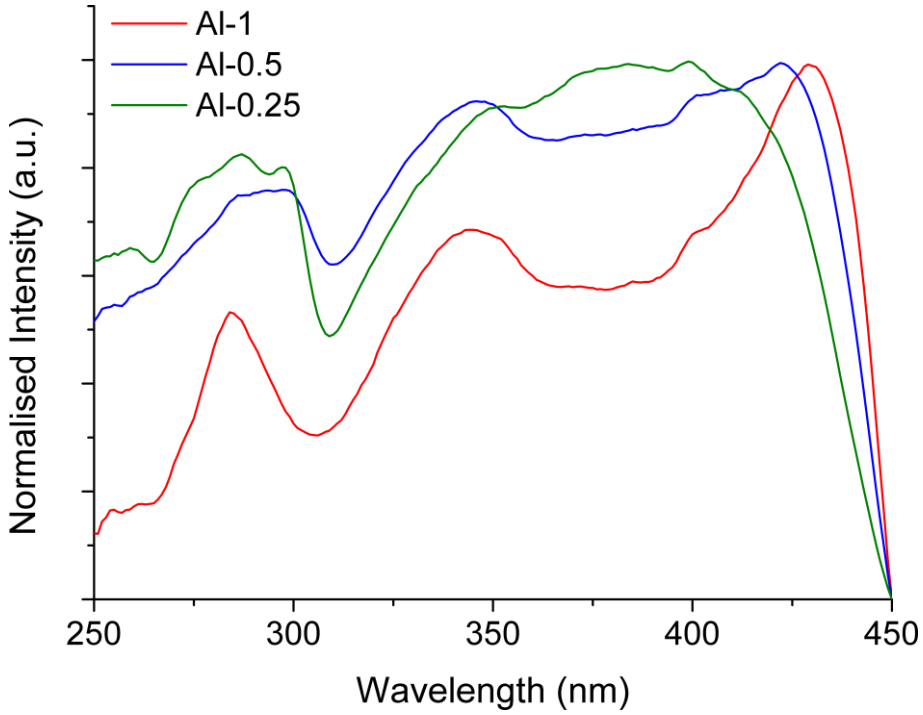

Figure S17. *Excitation spectra of* ***Al–1*** *(red),* ***Al–0.5*** *(blue) and* ***Al–0.25*** *(green).*

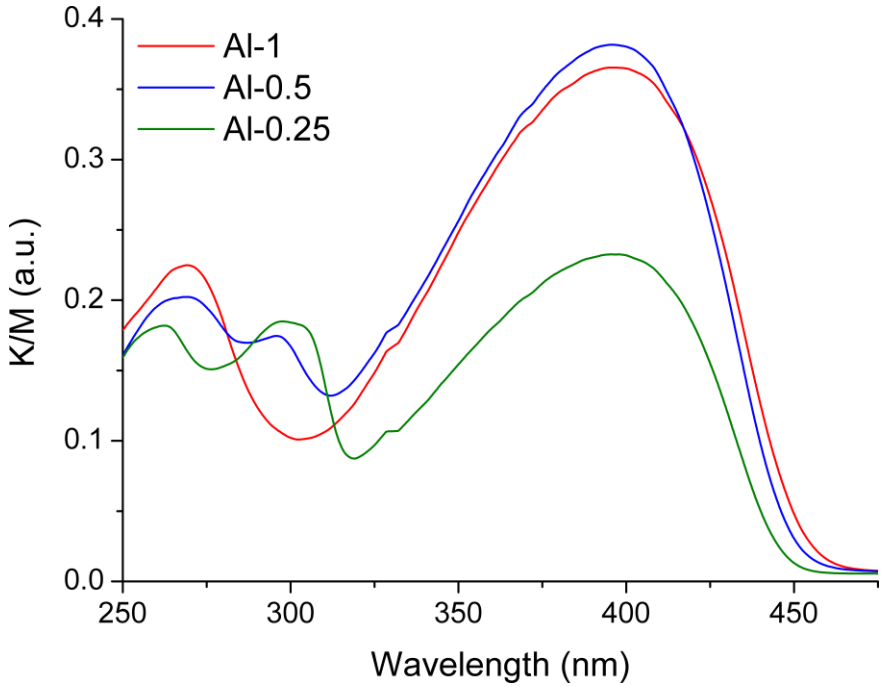

Figure S18. *Diffuse reflectance spectra of* ***Al–1*** *(red),* ***Al–0.5*** *(blue) and* ***Al–0.25*** *(green) calculated according to the Kubelka-Munk (K/M) model.*

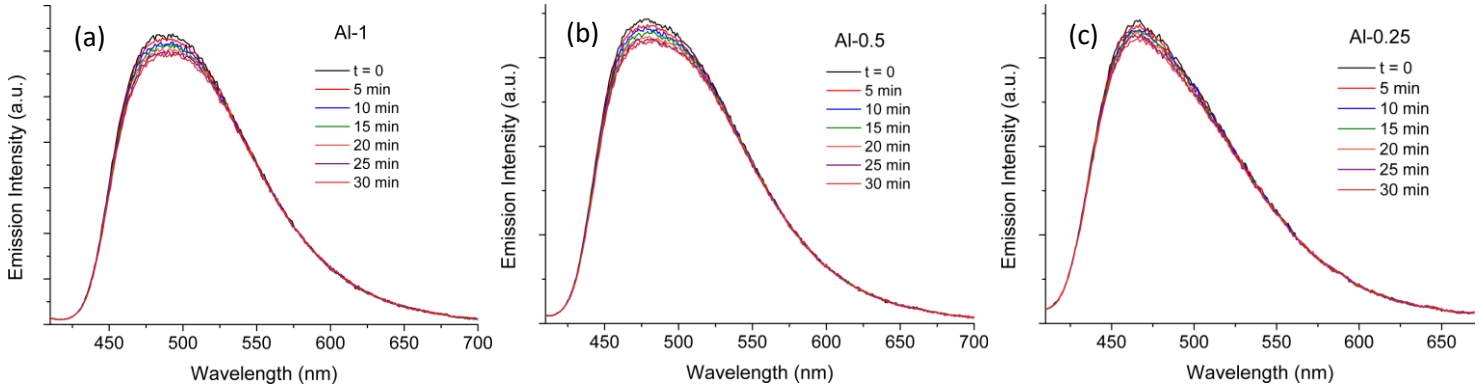

Figure S19. *Emission intensity of* ***Al–1*** *(a),* ***Al–0.5*** *(b) and* ***Al–0.25*** *(c) measured in the span of 30 minutes.*

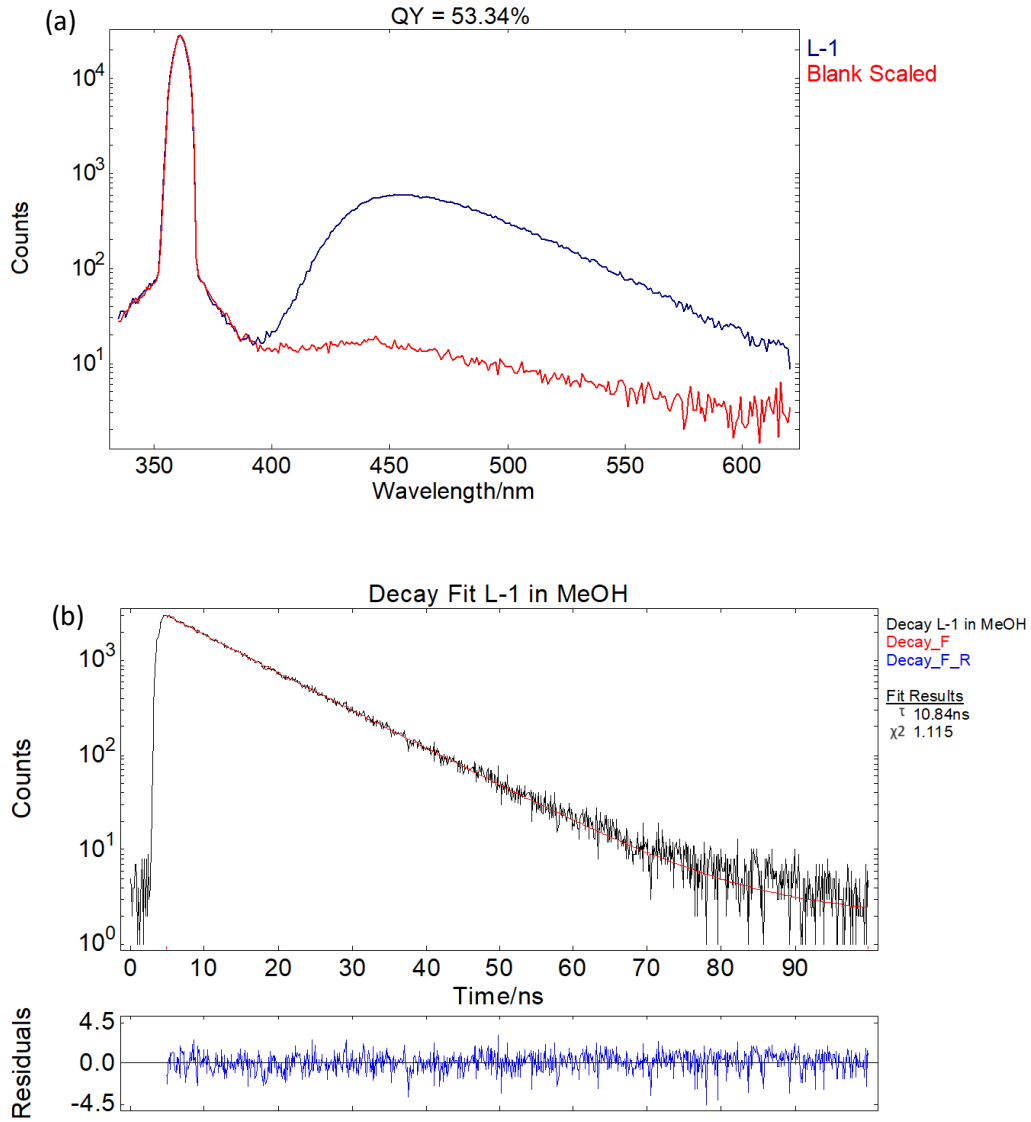

Figure S20. *Emission quantum yield (a) and time-resolved emission study (b) of ligand* ***L–1*** *in MeOH solution.*

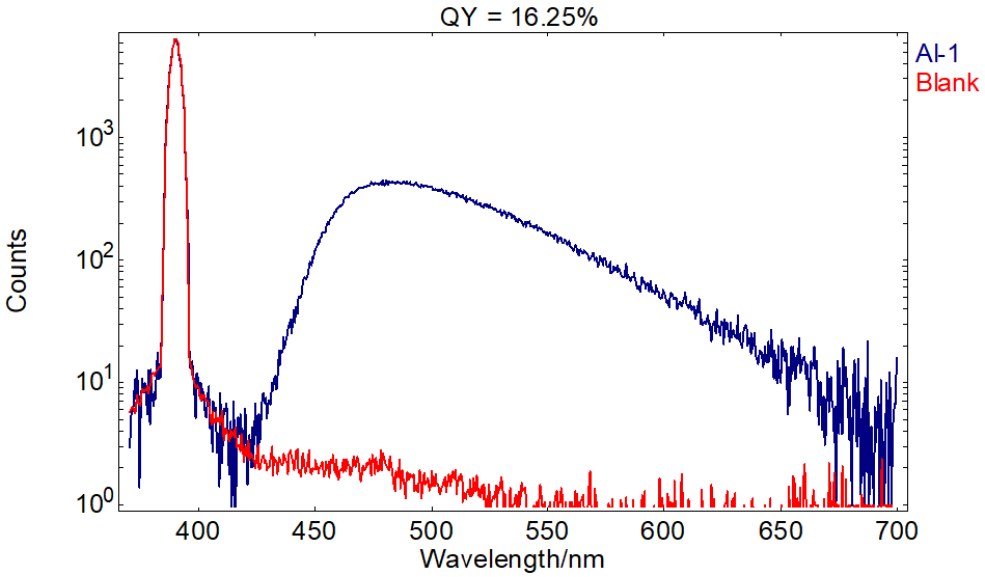

Figure S21. *Emission quantum yield of* ***Al–1****.*

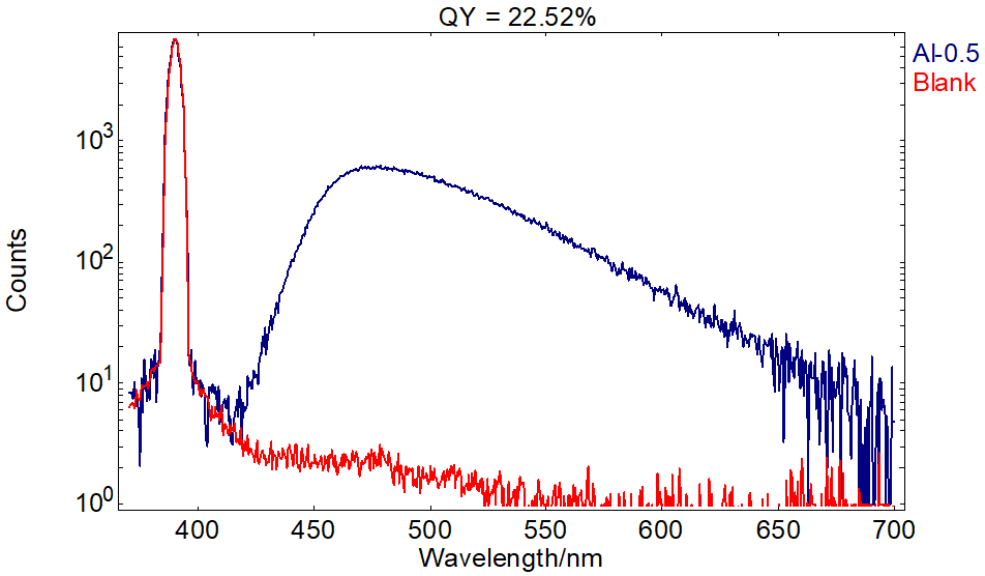

Figure S22. *Emission quantum yield of* ***Al–0.5****.*

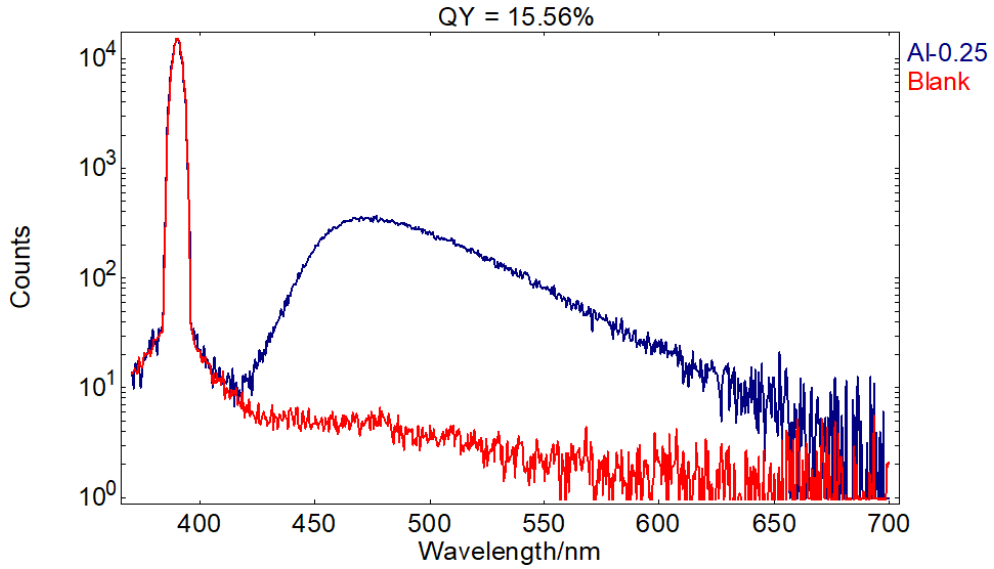

Figure S23. *Emission quantum yield of* ***Al–0.25****.*

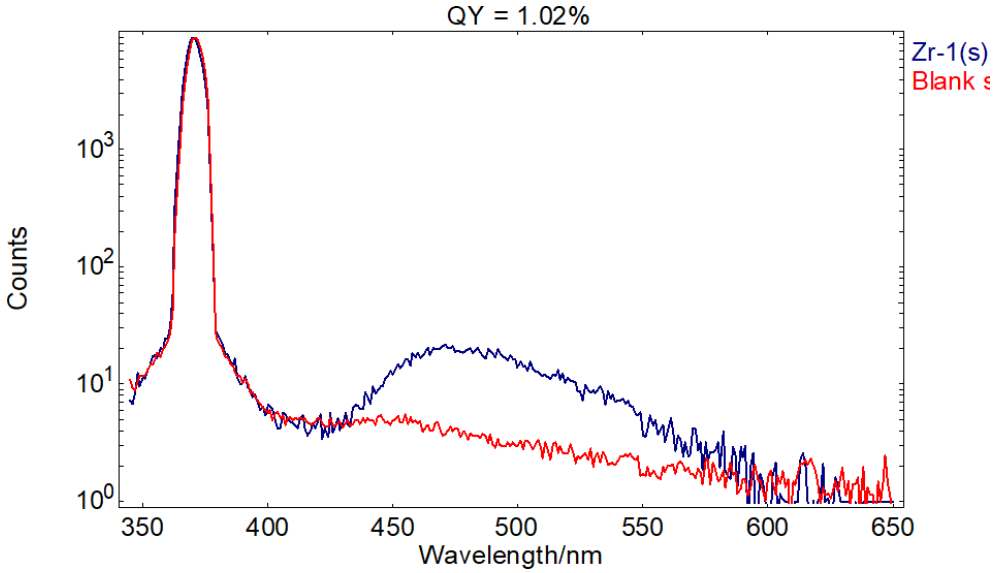

Figure S24. *Emission quantum yield of* ***Zr–1****.*

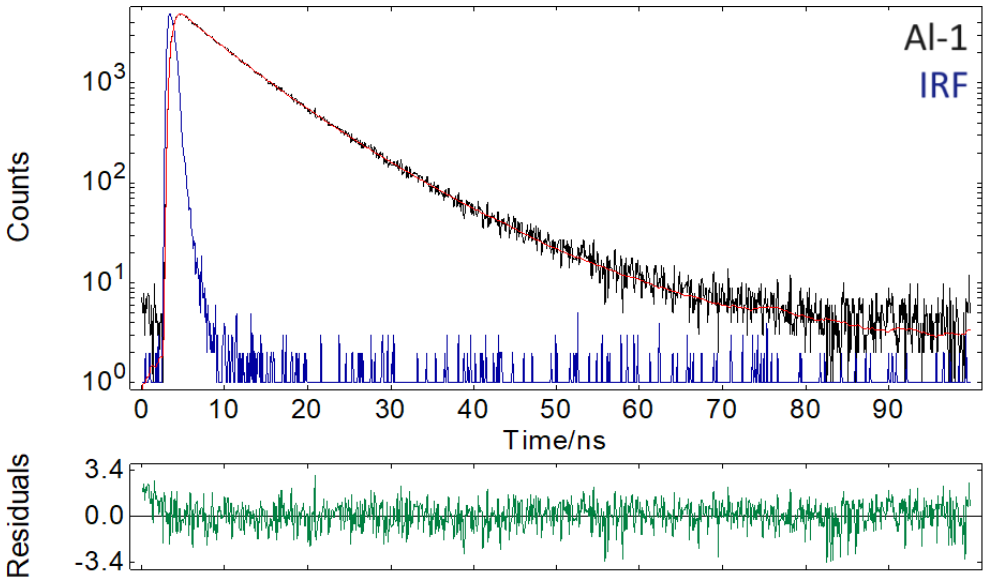

Figure S25. *Time-resolved emission study of* ***Al–1*** *showing experimental data (black), instrument response (blue), exponential fitting (red) and residuals (green). See Table 1 for fitting results.*

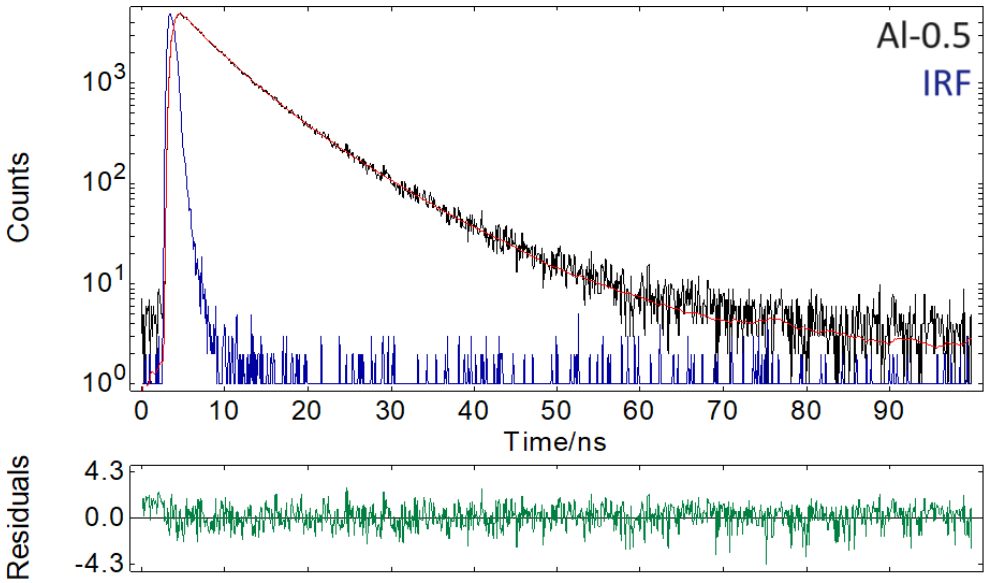

Figure S26. *Time-resolved emission study of* ***Al–0.5*** *showing experimental data (black), instrument response (blue), exponential fitting (red) and residuals (green). See Table 1 for fitting results.*

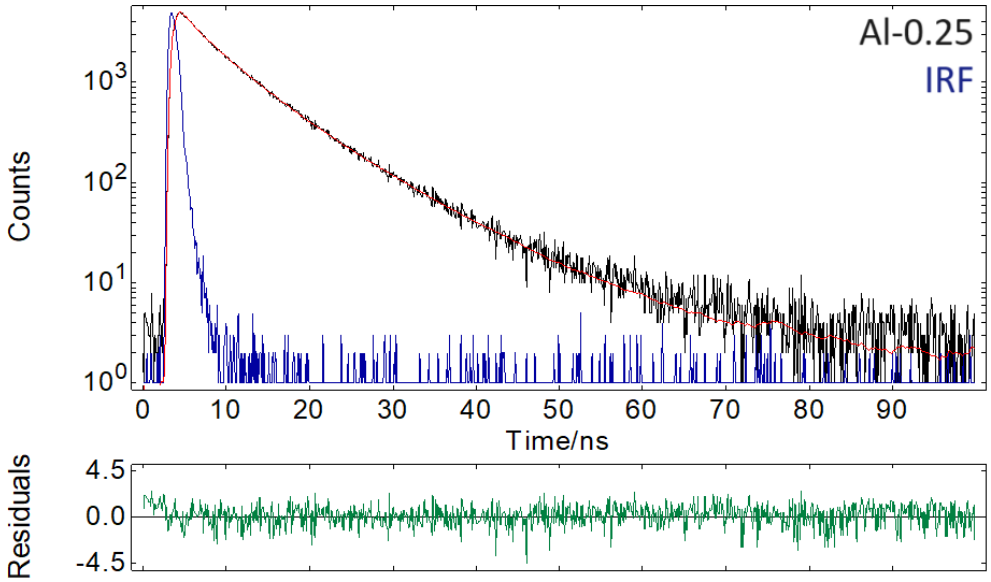

Figure S27. *Time-resolved emission study of* ***Al–0.25*** *showing experimental data (black), instrument response (blue), exponential fitting (red) and residuals (green). See Table 1 for fitting results.*

Detection of analytes in vapour phase

In a typical experiment, 1 mg of finely ground MOF powder was dispersed in 1 ml of MeOH, and the resulting suspension was sonicated for *ca*. 10 min. Then, 200 µL of the suspension was transferred on a cover glass slide (10 mm × 30 mm). The MeOH was evaporated after about 5 minutes to afford a thin MOF layer and the sample was activated by heating the loaded glass at 120 °C for 24 h. Likewise, in the case of MOF@HEC films, the coated glasses were activated at 120 °C for 24 h. Prior to the fluorescence experiments, solid analyte (5 mg) or liquid analyte (100 µL) was deposited at the bottom of a quartz cuvette and a piece of cotton wool or gauze was placed above it. The cuvette was then stoppered and kept at a constant temperature (25 °C) overnight to ensure that analyte vapour pressure reached equilibrium. After activation, the emission spectrum of the MOF- or MOF@HEC-loaded glass was recorded multiple times in the span of 30 minutes to ensure signal stability. Finally, the glass was carefully placed within the quartz cuvette containing the analyte –on top of the layer of cotton wool or gauze to ensure no direct contact between MOF and analyte– and after specified exposure time, the emission spectrum was recorded. The quenching efficiency (%) was calculated using the formula:

$$Q\% = \frac{I_0 - I}{I_0} \times 100 \quad \textbf{(S3)}$$

where I_0 and I are the integrated fluorescence intensities of the MOF sample at the start and the end of exposure, respectively.

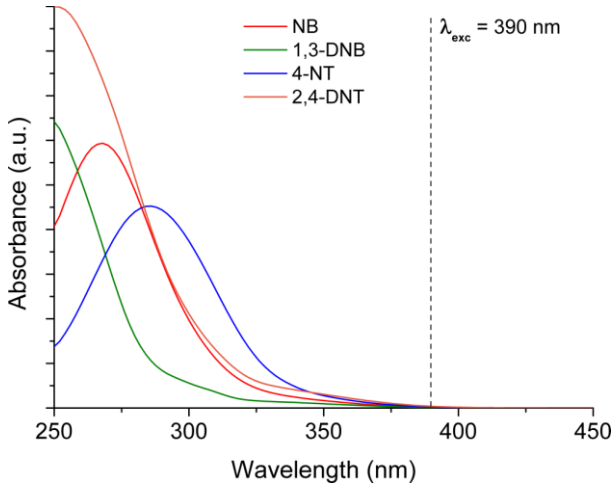

Figure S28. *UV-Vis spectra of analytes NB, 1,3-DNB, 4-NT, 2,4-DNT.*

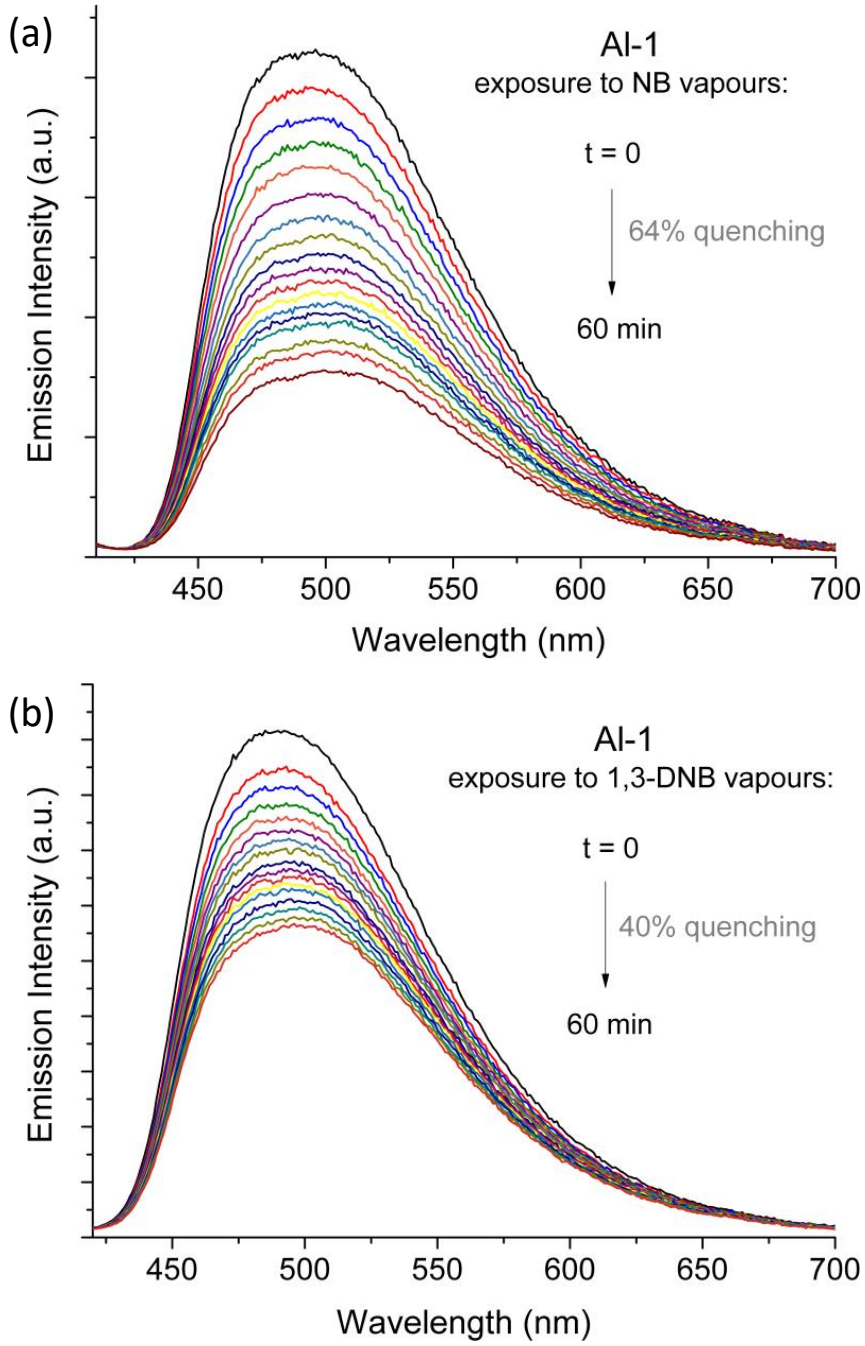

Figure S29. *Emission quenching of* ***Al–1*** *upon exposure to vapours of (a) NB and (b) 1,3-DNB.*

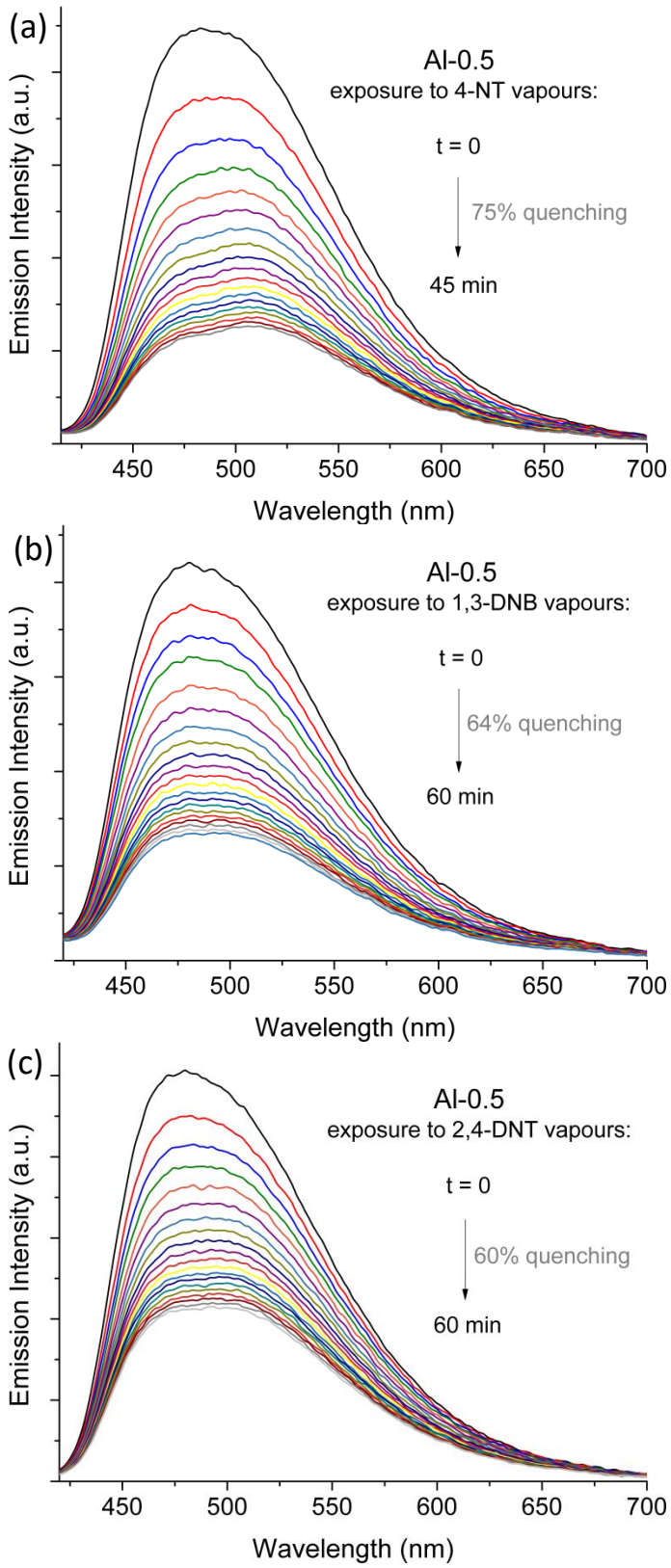

Figure S30. *Emission quenching of* ***Al–0.5*** *upon exposure to vapours of (a) 4-NT, (b) 1,3-DNB and (c) 2,4-DNT.*

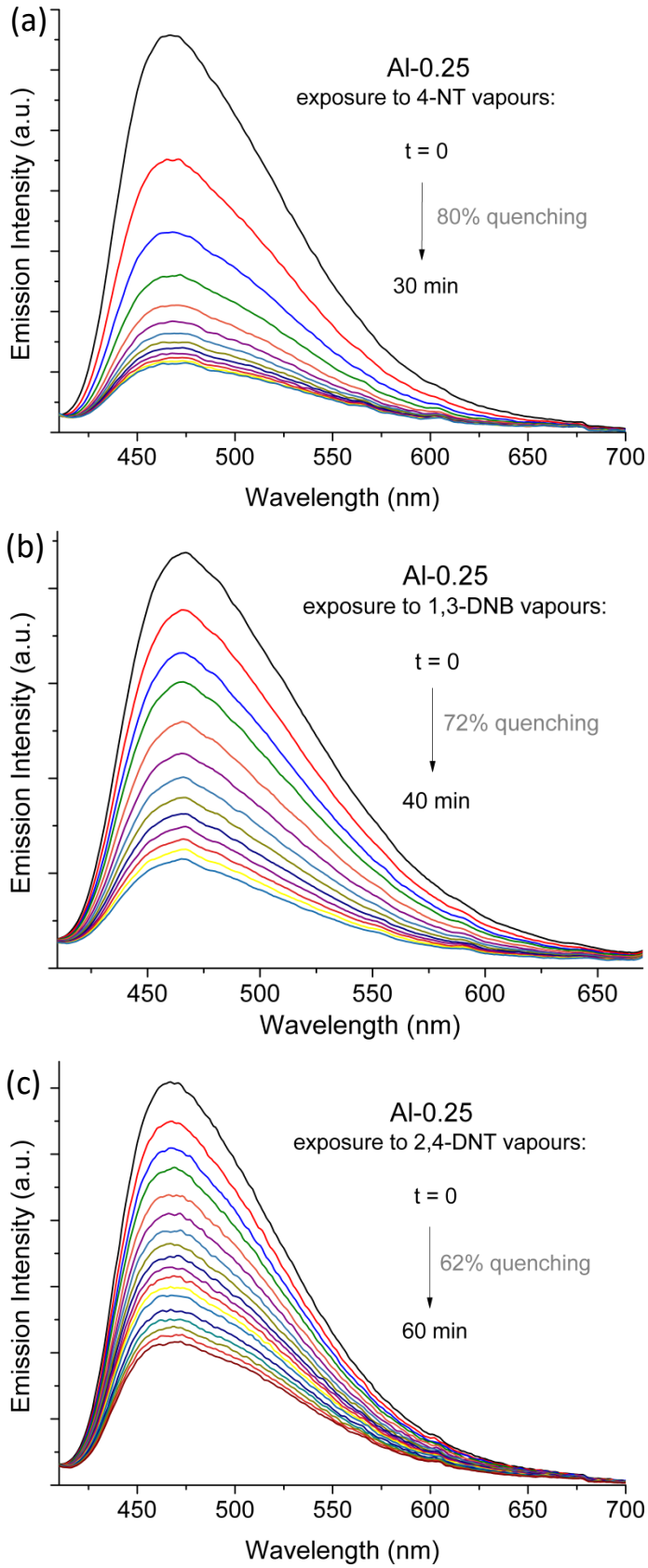

Figure S31. *Emission quenching of* ***Al–0.25*** *upon exposure to vapours of (a) 4-NT, (b) 1,3-DNB and (c) 2,4-DNT.*

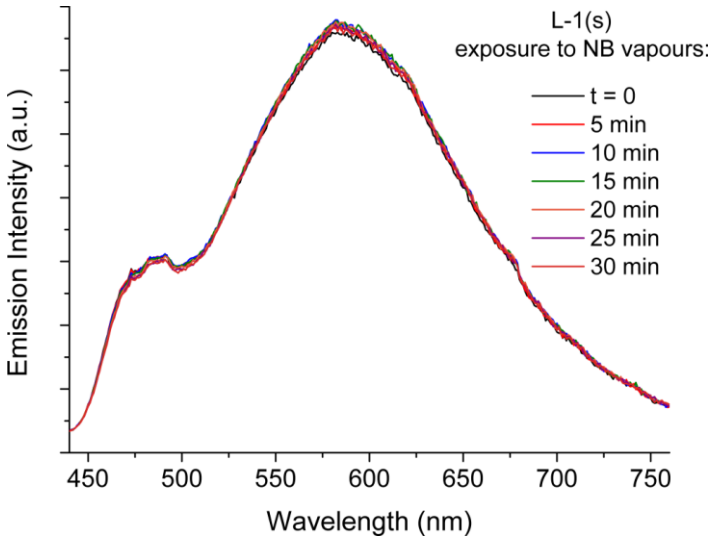

Figure S32. *Emission intensity of ligand* ***L–1****(s) upon exposure to vapours of NB.*

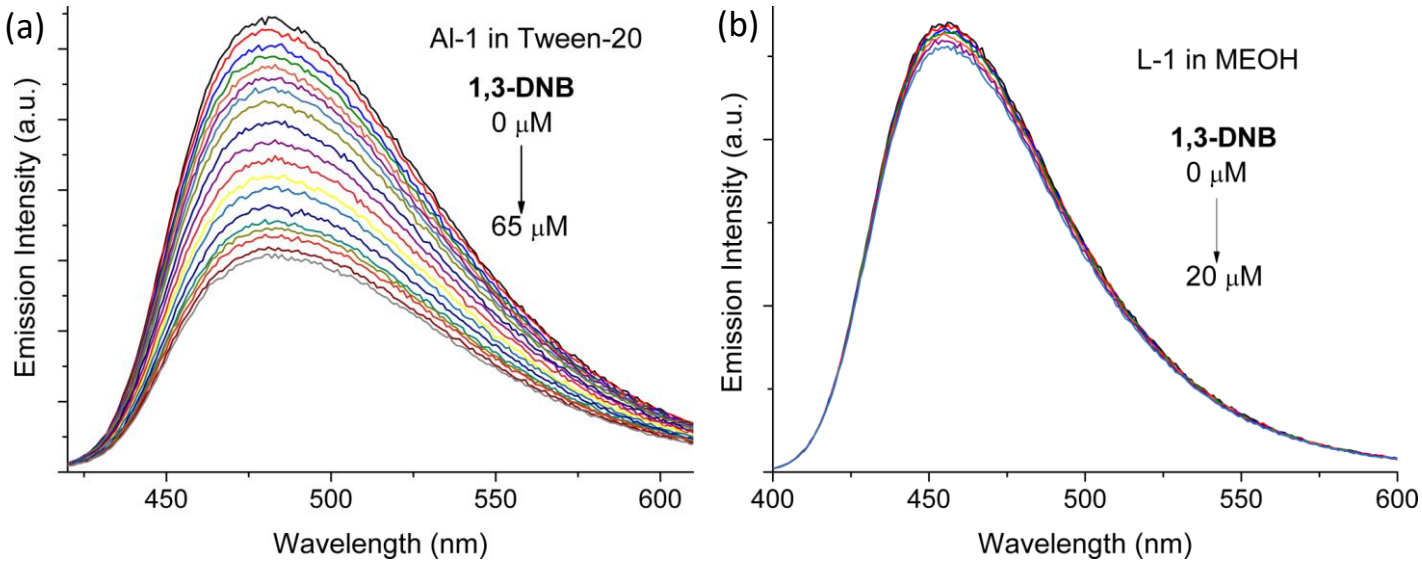

Figure S33. *Fluorescence titrations on (a)* ***Al–1*** *suspended in Tween-20 (2 mL, 0.05 mg* mL^{-1}*) (*λ_{exc} *= 400 nm) and (b) MeOH solution of* ***L–1*** *(*10^{-4} *M) (*λ_{exc} *= 360 nm) upon gradual addition of solutions of 1,3-DNB (*5×10^{-4} *M).*

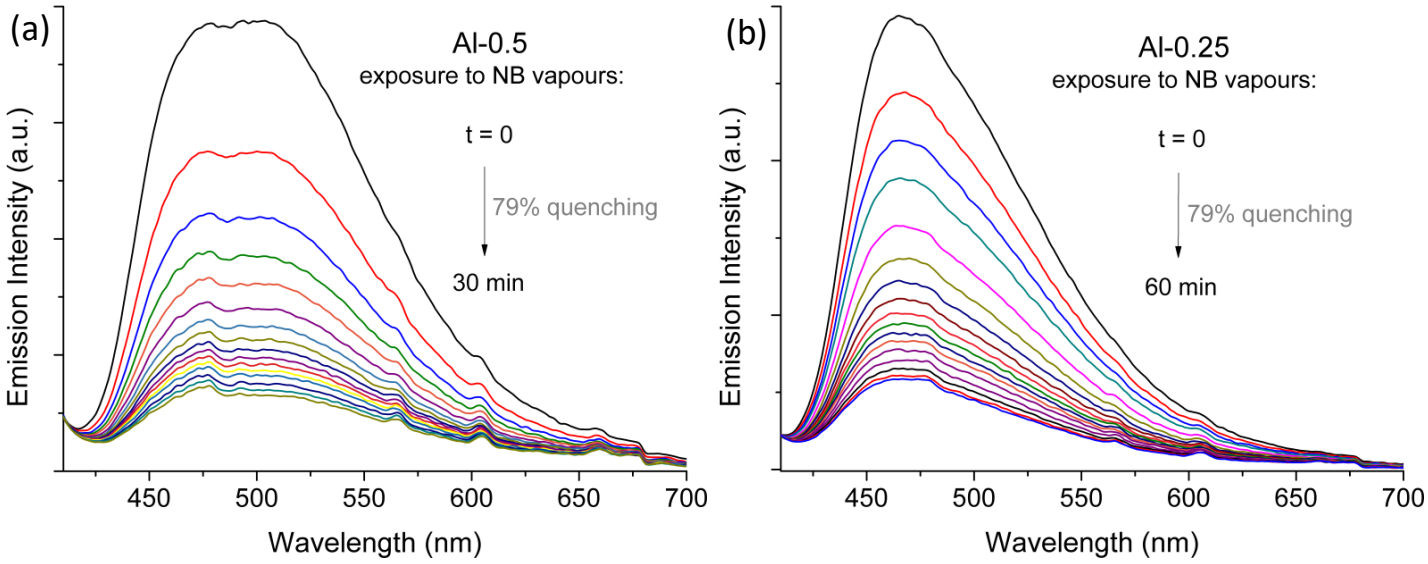

Figure S34. *Emission quenching of regenerated materials, thermally treated at 120 °C overnight (a)* ***Al–0.5*** *and (b)* ***Al–0.25*** *upon exposure to vapours of NB.*

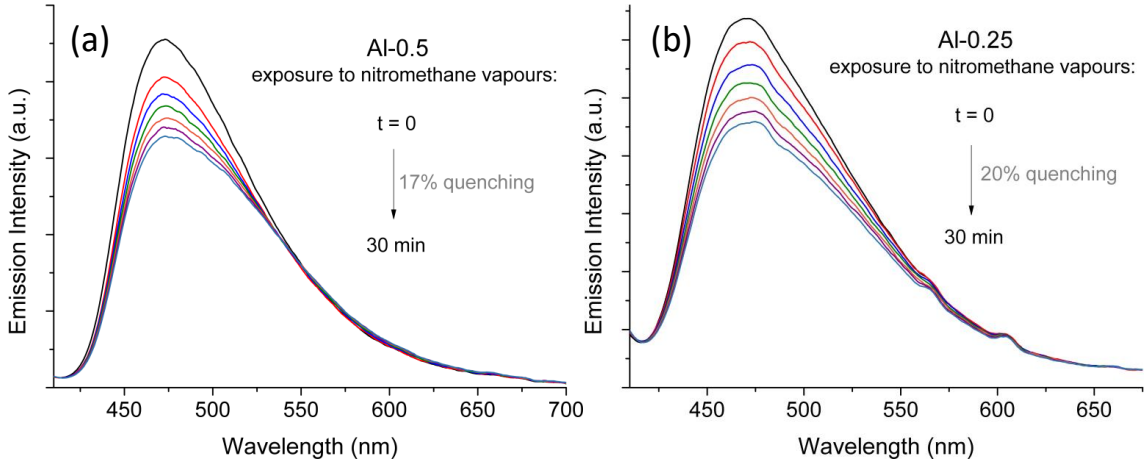

Figure S35. *Emission quenching of (a)* ***Al–0.5*** *and (b)* ***Al–0.25*** *upon exposure to vapours of nitromethane.*

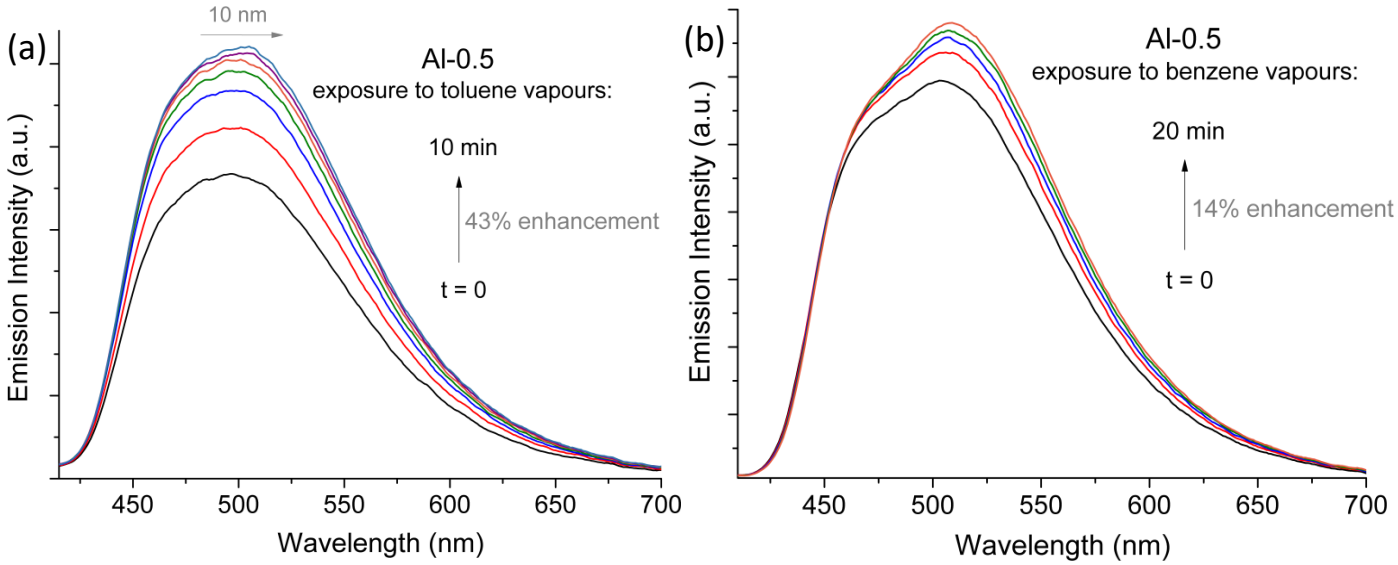

Figure S36. *Emission enhancement of* ***Al–0.5*** *upon exposure to vapours of (a) toluene and (b) benzene.*

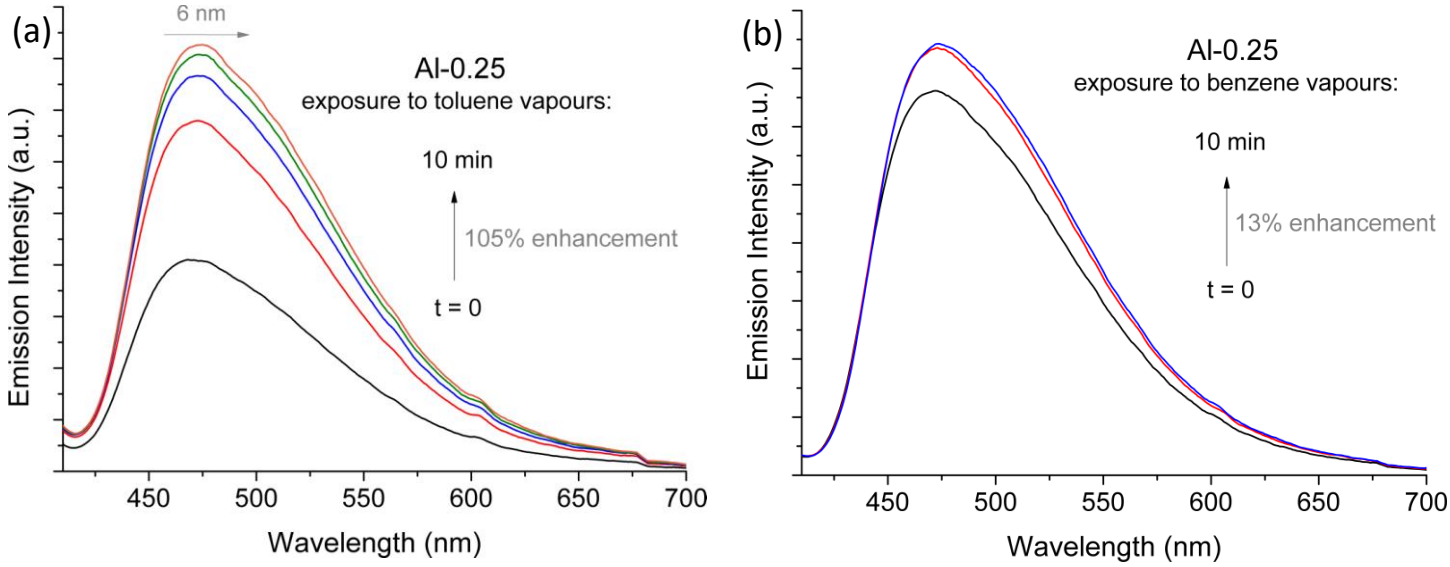

Figure S37. *Emission enhancement of* ***Al–0.25*** *upon exposure to vapours of (a) toluene and (b) benzene.*

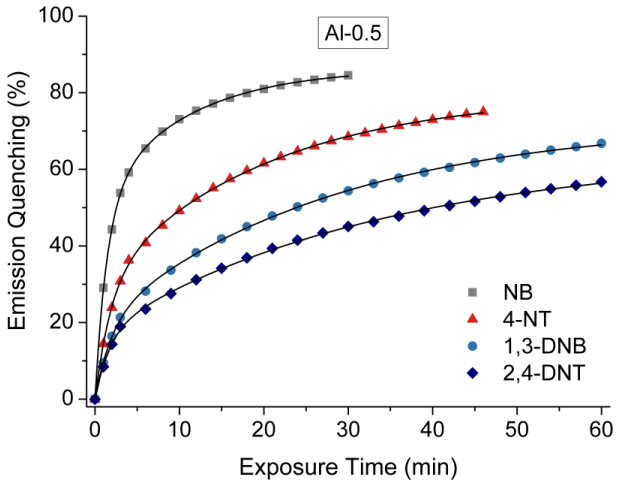

Equation	y = A1*exp(-x/t1) + A2*exp(-x/t2) + y0		**NB**
Adj. R-Square	1		
		Value	Standard Error
B	y0	86.33	0.28
B	A1	-51.13	0.76
B	t1	1.44	0.03
B	A2	-35.15	0.57
B	t2	10.46	0.37

Equation	y = A1*exp(-x/t1) + A2*exp(-x/t2) + y0		**4-NT**
Adj. R-Square	1		
		Value	Standard Error
F	y0	79.73	0.54
F	A1	-29.73	0.77
F	t1	1.87	0.08
F	A2	-50.12	0.47
F	t2	19.91	0.72

Equation	y = A1*exp(-x/t1) + A2*exp(-x/t2) + y0		**1,3-DNB**
Adj. R-Square	1		
		Value	Standard Error
D	y0	72.45	0.56
D	A1	-19.45	0.62
D	t1	1.89	0.11
D	A2	-53.08	0.39
D	t2	27.7	0.87

Equation	y = A1*exp(-x/t1) + A2*exp(-x/t2) + y0		**2,4-DNT**
Adj. R-Square	1		
		Value	Standard Error
H	y0	64.09	0.92
H	A1	-47.32	0.6
H	t1	33.1	1.62
H	A2	-16.93	0.67
H	t2	1.67	0.12

Figure S38. *Exponential decay fit (black lines) on quenching data of* ***Al–0.5*** *upon exposure to vapours of NB, 4-NT, 1,3-DNB, 2,4-DNT and the corresponding fitting results.*

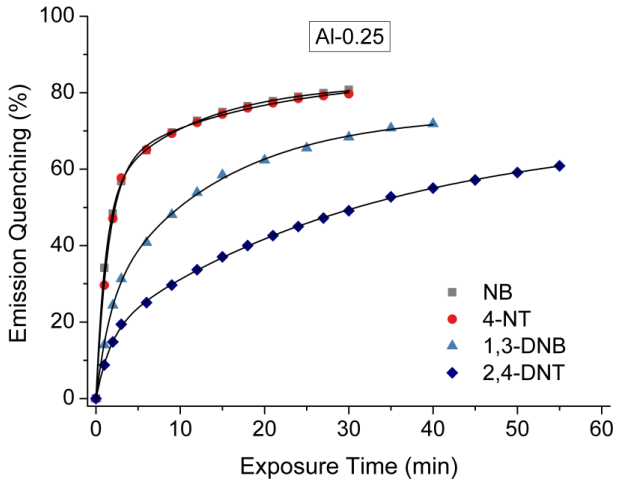

Equation	y = A1*exp(-x/t1) + A2*exp(-x/t2) + y0		**NB**
Adj. R-Square	1		
		Value	Standard Error
B	y0	82.51	0.61
B	A1	-29.13	0.83
B	t1	11.26	0.92
B	A2	-53.32	1.2
B	t2	1.13	0.04

Equation	y = A1*exp(-x/t1) + A2*exp(-x/t2) + y0		**4-NT**
Adj. R-Square	1		
		Value	Standard Error
D	y0	84.24	3.51
D	A1	-60.35	2.99
D	t1	1.48	0.1
D	A2	-24.25	1.9
D	t2	17.11	6.72

Equation	y = A1*exp(-x/t1) + A2*exp(-x/t2) + y0		**1,3-DNB**
Adj. R-Square	1		
		Value	Standard Error
F	y0	74.49	1.15
F	A1	-25.29	2.63
F	t1	1.65	0.23
F	A2	-49.4	1.91
F	t2	14.02	1.39

Equation	y = A1*exp(-x/t1) + A2*exp(-x/t2) + y0		**2,4-DNT**
Adj. R-Square	1		
		Value	Standard Error
H	y0	70.49	0.89
H	A1	-16.94	0.55
H	t1	1.68	0.1
H	A2	-53.68	0.59
H	t2	32.12	1.27

Figure S39. *Exponential decay fit (black lines) on quenching data of* ***Al–0.25*** *upon exposure to vapours of NB, 4-NT, 1,3-DNB, 2,4-DNT and the corresponding fitting results.*

Table S2. *Fluorescence lifetimes of* ***Al–1, Al–0.5*** *and* ***Al–0.25*** *as calculated from exponential fitting of time-resolved emission studies.*

Sample	τ_1 (ns)		τ_2 (ns)		τ_3 (ns)		χ^2
Al-1	1.90±0.87	17.55%	4.36±0.23	59.43%	11.65±0.37	23.02%	1.172
Al-1 + NB	0.63±0.03	23.84%	2.86±0.08	48.30%	9.56±0.19	27.86%	1.147
Al-1 + 1,3-DNB	1.23±0.06	22.73%	3.85±0.12	58.03%	11.23±0.36	19.24%	1.258
Al-0.5	1.89±0.18	13.58%	4.95±0.24	58.01%	11.59±0.38	28.41%	1.061
Al-0.5 + NB	0.32±0.01	28.18%	2.25±0.06	38.32%	8.30±0.15	33.49%	1.086
Al-0.5 + 4-NT	0.52±0.10	28.20%	2.48±0.07	41.28%	9.45±0.15	30.53%	1.211
Al-0.5 + 1,3-DNB	1.05±0.04	27.51%	3.53±0.01	47.95%	10.08±0.27	24.54%	1.147
Al-0.5 + 2,4-DNT	1.01±0.04	22.23%	3.34±0.12	46.03%	10.03±0.19	31.74%	1.251
Al-0.5@HEC	1.50±0.18	9.46%	4.31±0.18	60.67%	10.10±0.29	29.87%	1.143
Al-0.5@HEC+NB	0.88±0.05	15.91%	3.43±0.09	60.05%	9.86±0.24	24.04%	1.092
Al-0.25	1.68±0.23	7.20%	4.88±0.29	42.09%	11.59±0.22	50.71%	1.072
Al-0.25 + NB	0.34±0.01	10.78%	3.16±0.19	26.85%	10.23±0.10	62.37%	1.135
Al-0.25 + 4-NT	0.81±0.03	14.58%	3.94±0.15	33.39%	11.63±0.16	52.03%	1.082
Al-0.25 + 1,3-DNB	0.81±0.04	13.54%	3.87±0.17	32.55%	10.59±0.14	53.91%	1.148
Al-0.25 + 2,4-DNT	1.05±0.04	17.97%	4.52±0.20	37.49%	11.00±0.20	44.54%	1.191
Al-0.25@HEC	1.18±0.12	9.09%	3.80±0.14	50.41%	10.16±0.17	40.51%	1.254
Al-0.25@HEC + NB	0.59±0.02	17.95%	3.18±0.07	51.63%	10.78±0.19	30.41%	1.091

Table S3. *Representative examples of luminescent MOF sensors for nitroaromatic vapours.*

LMOF	Analyte	Emission Quenching	λ_{exc} (nm)	$\lambda_{em,max}$ (nm)	Ref.
$[Mg_2(BDC)_2(BPNO)]\cdot 2DMF$	NB, NM, NE	95%, 92%, 83%	305	421	9
$[Mg_2(H_2O)4TCPP]\cdot DMF\cdot 5CH_3CN$	TNP	-	365	432	10
$[Zn_2(bpdc)_2(bpee)]\cdot 2DMF$	DMNB, 2,4-DNT	85%, 84%	320	420	11
$[Zn_2(oba)_2(bpy)]\cdot 3DMA$	various NACs	10-87%	280	420	12
[Zn3(bpdc)3(by)]·4DMF·H2O	NB, m-DNB, p-DNB, 2-NT, 2,4-DNT	84%, 18%, 9%, 46%, <9%	300	420	13
[Zn3(bpdc)3(2,2'dmbpy)]·4DMF·H2O		77%, 31%, 10%, 55%, 17%	320	388	
[Zn2(bpdc)2(bpe)]·2DMF		88%, 10%, <10%, 37%, <10%	330	450	
[Zn(bpdc)(bpe)]·DMF		72%, 10%, 10%, 10%, 10%	330	425	
$[Zn(ndc)(bpe)_{0.5}]$ (FAM-8)	various NACs	10-58%	330	425	14
$[Zn(ndc)(bpee)_{0.5}]$ (FAM-9)		10-70%	330	450	
$[Zn(ndc)(ted)_{0.5}]$ (FAM-10)		37-84%	340	420	
$[Zn(ndc)(bpy)_{0.5}]$ (FAM-11)		10-52%	300	450	
$[Zn_{1.5}(L)(H_2O)]\cdot 1.5benzene$	various NACs	39-86%	280	390	15
$[Zn_2(TCPPE)]$	NB, 2,4-DNT	>80%	365	535	16
[Zn(dcbpy)(DMF)]·DMF	DMNB, NB, p-NT, 2,4-DNT	12%, 11%, 9%, 8%	-	~470	17
[Zn(dcbpy)(DMF)]·DMF (mw)		46%, 11%, 9%, 8%			
$[Cd_2(btc)_2(H_2O)_2]$ nanotube	2,4-DNT	73%	315	400	18
$[NH_2(CH_3)_2]_2[Cd_{17}(L)_{12}(\mu_3\text{-}H_2O)_4(DMF)_2(H_2O)_2]\cdot solv$	NB	76%	290	360	19
$[Cd_3(L)(bipy)2\cdot 4DMA]_n$	NB	>90%	314	381	20
$([ACF]^+ + [Ru]^{2+})@(Me_2NH_2)3Cd_{0.5}[Cd_3L_2]\cdot 6DMF\cdot 9H_2O$	various NACs, various temperatures		365	490	21
$[In_2L][NH_2(CH_3)_2]_2\cdot(DMF)_4(H_2O)_{16}$	NB, 1,3-DNB, 2,4-DNT	81%, 46%, 14%	280	360	22
$\{[Eu_2(TDC)_3(CH_3OH)_2]\cdot CH_3OH\}$	NB	>80%	325	615	23
[Tb(L)(OH)]·x(solv)	NB, 2-NT	90%, 80%	350	542	24
$[Tb_4(L)_6(H2O)_8]$	various NACs	up to 94%	360	543	25
Tb(BTC)@PMMA	TNP, TNT	69%, 29%	305	490, 543	26
$[Dy(dcbpy)(DMF)_2(NO_3)]$	NB, p-NT	13%, 3%	-	~480	17
$[Pb_3(L)_3(H_2O)_2]\cdot 10DMF\cdot 6.5H_2O$	various NACs, various temperatures		365	450	27
$FRS@[Pb_3(L)_3(H_2O)_2]\cdot 10DMF\cdot 6.5H_2O$				450, 540	
$[Ru]^{2+}@[Pb_3(L)_3(H_2O)_2]\cdot 10DMF\cdot 6.5H_2O$				450, 540, 600	

1 A. Chatz-Giachia, A. E. Psalti, A. D. Pournara, M. J. Manos, C. Pappa, K. Triantafyllidis and T. Lazarides, *J. Mater. Chem. C*, 2022, **10**, 12307–12315.

2 S. Brunauer, P. H. Emmett and E. Teller, *J. Am. Chem. Soc.*, 1938, **60**, 309–319.

3 T. K. Trung, P. Trens, N. Tanchoux, S. Bourrelly, P. L. Llewellyn, S. Loera-Serna, C. Serre, T. Loiseau, F. Fajula and G. Férey, *J. Am. Chem. Soc.*, 2008, **130**, 16926–16932.

4 T. Ahnfeldt, D. Gunzelmann, T. Loiseau, D. Hirsemann, J. Senker, G. Férey and N. Stock, *Inorg. Chem.*, 2009, **48**, 3057–3064.

5 X. Cheng, A. Zhang, K. Hou, M. Liu, Y. Wang, C. Song, G. Zhang and X. Guo, *Dalton Trans.*, 2013, **42**, 13698–13705.

6 A. Abramova, N. Couzon, M. Leloire, P. Nerisson, L. Cantrel, S. Royer, T. Loiseau, C. Volkringer and J. Dhainaut, *ACS Appl. Mater. Interfaces.*, 2022, **14**, 10669–10680.

7 T. Loiseau, C. Serre, C. Huguenard, G. Fink, F. Taulelle, M. Henry, T. Bataille and G. Férey, *Chem. Eur. J.*, 2004, **10**, 1373–1382.

8 J. M. Chin, E. Y. Chen, A. G. Menon, H. Y. Tan, A. T. S. Hor, M. K. Schreyer and J. Xu, *CrystEngComm*, 2013, **15**, 654–657.

9 D. Liu, X. Liu, Y. Liu, Y. Yu, F. Chen and C. Wang, *Dalton Trans.*, 2014, **43**, 15237–15244.

10 L. Wang, W. Chen, W. Song, J. Tian, J. Sun, L. Wen, C. Sun, X. Wang, Z. Su and G.-G. Shan, *Chin. Chem. Lett.*, 2023, **34**, 107291.

11 A. Lan, K. Li, H. Wu, D. H. Olson, T. J. Emge, W. Ki, M. Hong and J. Li, *Angew. Chem. Int. Ed.*, 2009, **48**, 2334–2338.

12 S. Pramanik, C. Zheng, X. Zhang, T. J. Emge and J. Li, *J. Am. Chem. Soc.*, 2011, **133**, 4153–4155.

13 S. Pramanik, Z. Hu, X. Zhang, C. Zheng, S. Kelly and J. Li, *Chem. Eur. J.*, 2013, **19**, 15964–15971.

14 D. Banerjee, Z. Hu, S. Pramanik, X. Zhang, H. Wang and J. Li, *CrystEngComm*, 2013, **15**, 9745–9750.

15 A. K. Chaudhari, S. S. Nagarkar, B. Joarder and S. K. Ghosh, *Cryst. Growth Des.*, 2013, **13**, 3716–3721.

16 X.-G. Liu, H. Wang, B. Chen, Y. Zou, Z.-G. Gu, Z. Zhao and L. Shen, *Chem. Commun.*, 2015, **51**, 1677–1680.

17 M. Jurcic, W. J. Peveler, C. N. Savory, D. O. Scanlon, A. J. Kenyon and I. P. Parkin, *J. Mater. Chem. A*, 2015, **3**, 6351–6359.

18 R. Li, Y.-P. Yuan, L.-G. Qiu, W. Zhang and J.-F. Zhu, *Small*, 2012, **8**, 225–230.

19 D. Tian, Y. Li, R.-Y. Chen, Z. Chang, G.-Y. Wang and X.-H. Bu, *J. Mater. Chem. A*, 2014, **2**, 1465–1470.

20 F.-Y. Yi, Y. Wang, J.-P. Li, D. Wu, Y.-Q. Lan and Z.-M. Sun, *Mater. Horiz.*, 2015, **2**, 245–251.

21 H. Zhao, L. Di, S.-W. Wang, J.-J. Zhang, Z. Liu, W.-J. Fang, S.-Q. Liu, J. Ni and X.-D. Song, *Sens. Actuators B: Chem.*, 2021, **328**, 129025.

22 Y.-S. Xue, Y. He, L. Zhou, F.-J. Chen, Y. Xu, H.-B. Du, X.-Z. You and B. Chen, *J. Mater. Chem. A*, 2013, **1**, 4525–4530.

23 F. Zhang, Y. Wang, T. Chu, Z. Wang, W. Li and Y. Yang, *Analyst*, 2016, **141**, 4502–4510.

24 J. Qin, B. Ma, X.-F. Liu, H.-L. Lu, X.-Y. Dong, S.-Q. Zang and H. Hou, *J. Mater. Chem. A*, 2015, **3**, 12690–12697.

25 X. Wang, J.-L. Li, C. Jiang, P. Hu, B. Li, T. Zhang and H.-C. Zhou, *Chem. Commun.*, 2018, **54**, 13271–13274.

26 F. G. Moscoso, J. Almeida, A. Sousaraei, T. Lopes-Costa, A. M. G. Silva, J. Cabanillas-Gonzalez, L. Cunha-Silva and J. M. Pedrosa, *J. Mater. Chem. C*, 2020, **8**, 3626–3630.

27 J. Ni, S.-W. Wang, P.-P. Zhang, J.-J. Zhang, H. Zhao, E.-P. Tan, Z.-Y. Li, J. Chen and C. Xia, *Cryst. Growth Des.*, 2021, **21**, 207–217.